The Group VIA Calcium-Independent Phospholipase A_2 Participates in ER Stress-Induced INS-1 Insulinoma Cell Apoptosis by Promoting Ceramide Generation via Hydrolysis of Sphingomyelins by Neutral Sphingomyelinase†

Xiaoyong Lei, Sheng Zhang, Alan Bohrer, Shunzhong Bao, Haowei Song, and Sasanka Ramanadham*

Department of Medicine, Mass Spectrometry Resource, and Division of Endocrinology, Metabolism, and Lipid Research, Washington University School of Medicine, St. Louis, Missouri 63110

Received January 4, 2007; Revised Manuscript Received April 24, 2007

ABSTRACT: β-Cell mass is regulated by a balance between β-cell growth and β-cell death, due to apoptosis. We previously reported that apoptosis of INS-1 insulinoma cells due to thapsigargin-induced ER stress was suppressed by inhibition of the group VIA Ca^{2+}-independent phospholipase A_2 (iPLA$_2\beta$), associated with an increased level of ceramide generation, and that the effects of ER stress were amplified in INS-1 cells in which iPLA$_2\beta$ was overexpressed (OE INS-1 cells). These findings suggested that iPLA$_2\beta$ and ceramides participate in ER stress-induced INS-1 cell apoptosis. Here, we address this possibility and also the source of the ceramides by examining the effects of ER stress in empty vector (V)-transfected and iPLA$_2\beta$-OE INS-1 cells using apoptosis assays and immunoblotting, quantitative PCR, and mass spectrometry analyses. ER stress induced expression of ER stress factors GRP78 and CHOP, cleavage of apoptotic factor PARP, and apoptosis in V and OE INS-1 cells. Accumulation of ceramide during ER stress was not associated with changes in mRNA levels of serine palmitoyltransferase (SPT), the rate-limiting enzyme in *de novo* synthesis of ceramides, but both message and protein levels of neutral sphingomyelinase (NSMase), which hydrolyzes sphingomyelins to generate ceramides, were temporally increased in the INS-1 cells. The increases in the level of NSMase expression in the ER-stressed INS-1 cells were associated with corresponding temporal elevations in ER-associated iPLA$_2\beta$ protein and catalytic activity. Pretreatment with BEL inactivated iPLA$_2\beta$ and prevented induction of NSMase message and protein in ER-stressed INS-1 cells. Relative to that in V INS-1 cells, the effects of ER stress were accelerated and/or amplified in the OE INS-1 cells. However, inhibition of iPLA$_2\beta$ or NSMase (chemically or with siRNA) suppressed induction of NSMase message, ceramide generation, sphingomyelin hydrolysis, and apoptosis in both V and OE INS-1 cells during ER stress. In contrast, inhibition of SPT did not suppress ceramide generation or apoptosis in either V or OE INS-1 cells. These findings indicate that iPLA$_2\beta$ activation participates in ER stress-induced INS-1 cell apoptosis by promoting ceramide generation via NSMase-catalyzed hydrolysis of sphingomyelins, raising the possibility that this pathway contributes to β-cell apoptosis due to ER stress.

Diabetes mellitus is the most prevalent human metabolic disease, and it results from loss and/or dysfunction of β-cells in pancreatic islets. Type 1 diabetes mellitus is caused by autoimmune β-cell destruction (*1*), and apoptosis plays a prominent role in the loss of β-cells during the development of type 1 diabetes mellitus (*1*, *2*). Type 2 diabetes mellitus results from a progressive decline of β-cell function and chronic insulin resistance which is characterized by initial peripheral insulin resistance and compensatory hyperinsulinemia that is followed by a loss of β-cell function and frank hyperglycemia (*3*−*6*).

Autopsy studies indicate that the β-cell mass in obese type 2 diabetes mellitus patients is smaller than that in obese non-diabetic subjects (*7*−*9*), and recent studies demonstrated that the loss of β-cell function in non-obese type 2 diabetes mellitus is also associated with decreases in β-cell mass (*10*, *11*). β-Cell mass is regulated by a balance between β-cell growth, resulting from β-cell replication and neogenesis, and β-cell death, resulting from apoptosis (*12*, *13*). Findings for both rodent models of type 2 diabetes mellitus (*14*−*16*) and human type 2 diabetes mellitus (*10*, *11*) have now led to the conclusion that the decrease in β-cell mass in type 2 diabetes mellitus cannot be attributed to a reduced level of β-cell proliferation or neogenesis but to an increased level of β-cell apoptosis. This conclusion is also supported by observations from other studies (*17*−*20*). It is therefore important to understand the mechanisms underlying β-cell apoptosis if this process is to be prevented or delayed.

Agents that induce β-cell apoptosis (*21*) act via an extrinsic pathway involving interaction with death receptors residing in the plasma membrane or via an intrinsic pathway involving mitochondrial signaling (*22*, *23*). A third organelle gaining

† This work was supported by grants from the National Institutes of Health (RO1-69455, R37-DK34388, P01-HL57278, P41-RR00954, P60-DK20579, and P30-DK56341).

* To whom correspondence should be addressed: Department of Medicine, Washington University School of Medicine, Campus Box 8127, 660 S. Euclid Ave., St. Louis, MO 63110. Telephone: (314) 362-8194. Fax: (314) 362-7641. E-mail: sramanad@im.wustl.edu.

10.1021/bi700017z CCC: $37.00
Published on Web 08/09/2007

prominence as a participant in apoptosis is the endoplasmic reticulum (ER)[1] (*22*−*26*). In addition to serving as a cellular Ca^{2+} store, the ER is the site where secretory proteins are synthesized, assembled, folded, and post-translationally modified. Interruption of any of these functions can lead to production of malfolded proteins that require rapid degradation. An imbalance between the load of client proteins on the ER and the ER's ability to process the load results in ER stress (*27*, *28*). Prolonged ER stress promotes induction of stress factors and activation of caspase-12, localized in ER (*23*, *25*, *26*, *29*), and can subsequently lead to apoptotic cell death. Downstream, all three pathways activate caspase-3, a protease that is central to execution of apoptosis (*30*). Being a site for Ca^{2+} storage, the ER responds to various stimuli to release Ca^{2+} and is therefore extremely sensitive to changes in cellular homeostasis. A number of factors can induce ER stress, and this process is thought to be a cause of various diseases, including Alzheimer's and Parkinson's diseases (*31*).

The secretory function of β-cells endows them with a highly developed ER and heightens their susceptibility to ER stress. Mutations in genes encoding the ER stress transducer pancreatic ER kinase (PERK) (*32*) and the ER resident protein involved in degradation of malfolded ER proteins are linked to diminished β-cell health clinically (*33*, *34*). Further, in the Akita diabetic mouse, mutation in the *Ins2*^{C96Y} gene produces an abnormal insulin product that accumulates in the ER. This leads to an increased level of expression of the ER chaperone protein GRP78 (BiP) and the ER stress marker CHOP (*15*, *35*−*37*) and a progressive decrease in β-cell mass, due to β-cell apoptosis, and subsequent hyperglycemia ensues.

The SERCA inhibitor thapsigargin (*38*) induces ER stress and promotes caspase-12 cleavage (*22*, *25*) and apoptosis of neurons and insulin-releasing BRIN-BID11 cells (*22*) and Apaf-1 null cells (*26*). While SERCA inhibitors promote loss of ER Ca^{2+} stores, induction of MIN-6 cell apoptosis by these agents occurs by a pathway that does not require an increase in $[Ca^{2+}]_i$ but instead requires the generation of arachidonic acid metabolites (*39*). Thapsigargin-induced ER stress in pancreatic islets leads to hydrolysis of arachidonic acid from membrane phospholipids also by a Ca^{2+}-independent mechanism that is suppressed by a bromoenol lactone (BEL) suicide substrate inhibitor of Ca^{2+}-independent phospholipase A_2 (iPLA$_2\beta$) (*40*). These observations raised the possibility that iPLA$_2\beta$ participates in ER stress in β-cells.

The PLA$_2$s are a diverse group of enzymes that catalyze hydrolysis of the *sn*-2 substituent from glycerophospholipid substrates to yield a free fatty acid and a 2-lysophospholipid (*41*). At present, the recognized PLA$_2$s are classified into 15 groups on the basis of their Ca^{2+} requirement for activation and sequence homology (*42*). Among the iPLA$_2$s is one that does not require Ca^{2+} for activity, is classified as a group VIA iPLA$_2$, and is designated as the β-isoform of iPLA$_2$ (iPLA$_2\beta$) (*43*−*45*), distinguishing it from the membrane-associated γ-isoform (iPLA$_2\gamma$) (*44*). The iPLA$_2\beta$ enzyme is activated by ATP and is inhibited by BEL (*46*). While in macrophage-like cells iPLA$_2\beta$ is proposed to be involved in phospholipid remodeling (*47*), iPLA$_2\beta$ is thought to participate in signal transduction in other cells (*48*−*53*), including β-cells (*43*, *46*, *54*, *55*).

Recent findings in non-β-cells suggested another role for iPLA$_2\beta$. Induction of human U937 promonocyte apoptosis by anti-Fas antibody is associated with hydrolysis of arachidonic acid from membrane phospholipids by a mechanism that is inhibited by BEL and that is not catalyzed by sPLA$_2$ or cPLA$_2$ (*56*). U937 cell apoptosis is also associated with cleavage of iPLA$_2\beta$ by caspase-3, and overexpression of this iPLA$_2\beta$ cleavage product amplifies both thapsigargin-induced arachidonic acid release and cell death (*57*). S49 lymphoma, PC12, and human coronary artery endothelial cell death induced by thapsigargin (*57*, *58*), polychlorinated biphenyls (*59*), and polycyclic aromatic hydrocarbons (*60*), respectively, are all reported to be suppressed by inhibitors of PLA$_2$, including BEL. Collectively, these observations suggest that iPLA$_2\beta$, in part, contributes to events that promote apoptosis, but the mechanism of its action has not yet been described.

Pancreatic islet β-cells and insulinoma cells express a iPLA$_2\beta$ activity that is sensitive to inhibition by BEL (*46*, *54*, *61*, *62*). We recently reported (*63*) that ER stress induces INS-1 insulinoma cell apoptosis and amplifies apoptosis of iPLA$_2\beta$-overexpressing (OE) INS-1 cells and that this is inhibited by BEL. An intriguing finding associated with induction of ER stress in INS-1 cell apoptosis was an increase in the level of ceramide generation that was also significantly amplified in OE INS-1 cells (*63*). Ceramides are lipid messengers that can suppress cell growth and induce apoptosis (*64*−*66*). In this study, we examine the relationship among ER stress, ceramide generation, iPLA$_2\beta$, and INS-1 cell apoptosis.

EXPERIMENTAL PROCEDURES

Materials. INS-1 insulinoma cells were provided by C. Newgard (Duke University Medical Center, Durham, NC). Other materials were obtained from the following sources: (16:0/[^{14}C]-18:2)GPC (PLPC, 55 mCi/mmol), rainbow molecular mass standards, and enhanced chemiluminescence reagent from Amersham (Arlington Heights, IL); SYBR Green PCR Kit from Applied Biosystems (Foster City, CA); brain and egg sphingomyelins, ceramide, and other lipid standards from Avanti Polar Lipids (Alabaster, AL); calnexin from BD Sciences (San Jose, CA); Coomassie reagent, SDS-PAGE supplies, and Triton X-100 from Bio-Rad (Hercules, CA); mitochondrial membrane potential detection kit from Cell Tech. Inc. (Mountain View, CA); retroviral vector siRNA reagents from Clontech (Mountain View, CA); paraformaldehyde from Electron Microscopy Sciences (Ft. Washington, PA); DNase-free RNase A from Gentra Systems Inc. (Minneapolis, MN); RT-PCR reagents from Invitrogen (Carlsbad, CA); Immobilin-P PVDF membrane from Millipore Corp. (Bedford, MA); complex IV antibody, Slow Fade light antifade kit from Molecular Probes (Eugene, OR); RNeasy kit from Qiagen Inc. (Valencia, CA); TUNEL kit from Roche Diagnostic Corp. (Indianapolis, IN); all other

[1] Abbreviations: BEL, bromoenol lactone suicide inhibitor of iPLA$_2\beta$; cPLA$_2$, group IV cytosolic phospholipase A_2; ER, endoplasmic reticulum; ESI, electrospray ionization; GPC, glycero-phosphocholine; iPLA$_2\beta$, β-isoform of group VIA calcium-independent phospholipase A_2; MitoMP, mitochondrial membrane potential; MS, mass spectrometry; NSMase, neutral sphingomyelinase; OE, iPLA$_2\beta$-overexpressing; PLA$_2$, phospholipase A_2; SEM, standard error of the mean; SERCA, sarcoendoplasmic reticulum Ca^{2+}-ATPase; SPT, serine palmitoyltransferase.

primary and secondary antibodies from Santa Cruz Biotechnology Inc. (Santa Cruz, CA); and ER isolation kit, protease inhibitor cocktail, common reagents, and salts from Sigma Chemical Co. (St. Louis, MO).

Preparation, Culture, and Treatment of Stably Transfected INS-1 Cells. A retroviral system (*46*, *67*) was used to stably transfect INS-1 cells with either empty retroviral vector (V INS-1 cells) or a vector construct containing iPLA$_2\beta$ cDNA (OE INS-1 cells), as described (*43*). The cells were cultured and passaged, as described (*68*), and grown to confluency in Petri dishes or flasks prior to treatment. The INS-1 cells were treated with either vehicle (DMSO, 0.50 μL/mL) alone or thapsigargin (1 μM) to induce ER stress and incubated for up to 24 h. In some studies, the cells were co-incubated with an inhibitor of iPLA$_2\beta$ (BEL, 10 μM), SPT (L-cycloserine, 1 μM), or NSMase (GW4869, 10 μM).

iPLA$_2\beta$ Activity Assay in V and OE INS-1 Cells. To verify that the INS-1 cells transfected with a construct containing iPLA$_2\beta$ cDNA expressed higher iPLA$_2\beta$ protein and catalytic activity, cytosol was prepared from these and V INS-1 cells, as described (*63*), and the protein concentration was determined using Coomassie reagent. Immunoreactive iPLA$_2\beta$ protein was visualized, as described below, and iPLA$_2\beta$ catalytic activity (in a 25 μg protein aliquot) in the absence and presence of ATP (10 mM) or BEL (1 μM) was assayed and quantitated, as described (*63*).

To examine whether expression of iPLA$_2\beta$ in the ER is affected by ER stress, the ER was prepared from vehicle- and thapsigargin-treated INS-1 cells, as described (*69*, *70*). Cells were harvested and washed twice (750 $\times$ *g* for 5 min at 4 °C) with 10 volumes of ice-cold phosphate-buffered saline. The cell pellet was suspended in 3 volumes of ice-cold isolation buffer [20 mM HEPES-KOH (pH 7.8), 250 mM sucrose, 1 mM EGTA, and 10 mM potassium chloride] supplemented with protease inhibitor cocktail (50 μL/mL). The cells were placed on ice for 15 min and then transferred to a Dounce homogenizer (Kimble/Kontes, Vineland, NJ) and disrupted by douncing 50 times on ice. The homogenate was then centrifuged (15,000 $\times$ *g* for 15 min at 4 °C), and the supernatant was separated from the mitochondria-containing pellet and further centrifuged (100,000 $\times$ *g* for 1 h at 4 °C), yielding an ER fraction. The pellet containing ER was then resuspended in HB buffer [40 mM Tris-HCl (pH 7.8), 250 mM sucrose, and 1 mM EGTA], sonicated, and the protein concentration was determined for iPLA$_2\beta$ activity and immunoblotting assays. Enrichment of the fraction with ER was verified by immunoblotting analyses for various organelle markers: calnexin (ER), complex IV (mitochondria), FTCD 58K-9 (Golgi), Oct-1 (nuclei), and Na^+/K^+-ATPase (membrane).

Immunoblotting Analyses. INS-1 cells were harvested at various times (0−24 h) following induction of ER stress and sonicated, and the homogenate was centrifuged (10,0000 $\times$ *g* for 1 h at 4 °C), yielding cytosol. An aliquot (containing 30 μg of protein) of homogenate, cytosol, ER, or mitochondria was analyzed by SDS-PAGE (8 or 15%), transferred onto Immobilin-P PVDF membranes, and processed for immunoblotting analyses, as described (*63*). The targeted proteins and the primary antibody concentrations were as follows: GRP78 and 1:500, CHOP and 1:500, PARP and 1:1000, iPLA$_2\beta$ (T-14) and 1:500, calnexin and 1:1000, complex IV and 1:2000, FTCD 58K-9 and 1:1000, Oct-1 and 1:1000, Na^+/K^+-ATPase and 1:2000, NSMase and 1:1000, and tubulin control and 1:2000. The secondary antibody concentration was 1:10000. Immunoreactive bands were visualized by enhanced chemiluminescence.

Assays for Apoptosis. To assess the incidence of apoptosis induced by ER stress TUNEL, DNA laddering, and mitochondrial membrane potential (MitoMP) analyses were performed as described below.

In Situ Detection of DNA Cleavage by TUNEL Staining. At various times, INS-1 cells were harvested and washed twice with ice-cold phosphate-buffered saline. The cells were then immobilized on slides by cytospin (*63*) and fixed with 4% paraformaldehyde (in PBS at pH 7.4 for 1 h at room temperature). The cells were then washed with PBS and incubated in permeabilization solution (0.1% Triton X-100 in 0.1% sodium citrate in phosphate-buffered saline for 30 min at room temperature). The permeabilization solution was then removed and TUNEL reaction mixture (50 μL) added, and the cells were incubated (1 h at 37 °C) in a humidified chamber. The cells were washed again with phosphate-buffered saline and counterstained with 1 μg/mL DAPI (4′,6′-diamidino-2-phenylindole) in phosphate-buffered saline for 10 min to identify cellular nuclei. The incidence of apoptosis was assessed under a fluorescence microscope using a FITC filter. Cells with TUNEL-positive nuclei were considered apoptotic. DAPI staining was used to determine the total number of cells in a field. A minimum of six fields per slide was used to calculate the percent of cells that were apoptotic.

DNA Laddering. Harvested INS-1 cells were washed three times with phosphate-buffered saline and resuspended in 500 μL of lysis buffer [100 mM Tris-HCl (pH 8.5), 5 mM EDTA, 0.2 M NaCl, 0.2% (w/v) SDS, and 0.2 mg/mL proteinase K]. After a 90 min incubation on ice, the lysates were centrifuged (10,000 $\times$ *g* for 10 min at 4 °C). The DNA in the supernatant was precipitated overnight with an equal volume of 100% (v/v) ethanol at −20 °C. The DNA precipitate was washed once with 70% ethanol and resuspended in 30 μL of 10 mM Tris-HCl/EDTA (pH 7.5) buffer supplemented with 200 μg/mL DNase-free RNase A. After incubation at 37 °C for 2 h, the DNA was analyzed using 2% agarose gel electrophoresis. DNA laddering, which reflects apoptosis-associated DNA fragmentation, was visualized using ethidium bromide staining under UV light.

Assessment of Mitochondrial Membrane Potential (MitoMP) by Flow Cytometry. Loss of MitoMP is an important step in the induction of cellular apoptosis (*71*). INS-1 cell MitoMP was measured using a commercial kit according to the manufacturer's instructions. Briefly, harvested cells were washed once with phosphate-buffered saline and resuspended in 100 μL of the same buffer ($\sim 10^5$ cells/mL). An aliquot (5 μL) of MitoFlow fluorescent reagent was added, and the cell suspension was incubated at 37 °C for 30 min. The cells were then transferred to fluorescence-activated cell sorting tubes and diluted 1:5 with buffer provided in the kit. Fluorescence in cells was analyzed by flow cytometry (BD Biosciences) at an excitation wavelength of 488 nm.

Ceramide Analyses by Electrospray Ionization (ESI) MS/MS. Lipids were extracted from INS-1 cells under acidic conditions, as described previously (*72*, *73*). Briefly, cells were harvested and gently pelleted, and extraction buffer [2:2:1.8 (v/v/v) chloroform/methanol/2% acetic acid mixture]

containing C8-ceramide (C8-ceramide, *m*/*z* 432) internal standard (IS, 500 ng) was added to the cellular pellet. After being vigorously vortexed, the mixture was centrifuged (800 $\times$ *g*) and the organic bottom layer was collected, concentrated to dryness under nitrogen, and reconstituted in a chloroform/methanol mixture (1:4) containing 10 pmol/μL LiOH. To measure ceramide content, ESI-MS/MS standard curves were generated from a series of samples containing a fixed amount of C8-ceramide standard and varied amounts of long-chain ceramide standards. The relative abundances of individual ceramide species, relative to the C8-ceramide internal standard, were measured by ESI-MS/MS scanning for constant neutral loss of 48, which reflects the elimination of formaldehyde and water from the $[M + Li]^+$ ion (*63*). This loss is characteristic of ceramide-Li^+ adducts upon low-energy collisionally activated dissociation ESI-MS/MS (*72*). Lipid phosphorus measurements were used to normalize individual ceramide molecular species.

Sphingomyelin Analyses by ESI-MS/MS. Sphingomyelins are formed by reaction of a ceramide with CDP-choline, and similar to glycerophosphocholine (GPC) lipids, they contain a phosphocholine as the polar head group. This feature of sphingomyelins facilitates identification of sphingomyelin molecular species by constant neutral loss scanning of trimethylamine $[[M + Li]^+ - N(CH_3)_3]$ or constant neutral loss of 59, as described (*74*). The prominent ions in the total ion current spectrum are those of the even mass PC molecular species, and these mask the odd mass sphingomyelin signals. Constant neutral loss of 59, however, facilitates emergence of signals for sphingomyelin species at odd *m*/*z* values, reflecting loss of nitrogen. Lipid extracts prepared as described above were used for the sphingomyelin analyses. In the absence of the availability of individual sphingomyelin species, sphingomyelin content in the samples was determined on the basis of standard curves generated using commercially available brain and egg sphingomyelins with a known percentage of each fatty acid constituent and 14:0/14:0-GPC (*m*/*z* 684, 8 μg) as an internal standard. Lipid phosphorus measurements were used to normalize individual sphingomyelin molecular species.

Quantitative RT-PCR. To assess the mRNA expression of key enzymes involved in ceramide-generating pathways, total RNA was isolated from INS-1 cells using an RNeasy kit (Qiagen Inc.). cDNA was then synthesized using a SuperScriptII kit (Invitrogen) and heat-inactivated (70 °C for 15 min). A reaction without reverse transcriptase was performed to verify the absence of genomic DNA. PCR amplifications were performed using the SYBR Green PCR kit (Invitrogen) in an ABI 7000 detection system (Applied Biosystems). The primers were designed on the basis of known rat sequences for neutral sphingomyelinase (NSMase), serine palmitoyltransferase (SPT), ceramidase, and internal control 18S provided in the GenBank database as entries AB047002, XM001053124, AF214647, and X01117, respectively. The sense and antisense primer sets were as follows: NSMase, ccggatgcacactacttcagaa and ggattgggtgtctggagaaca; SPT, caccgagcactatgggatca and cgagcgcattctccatgtta; ceramidase, tgaaagccaccttcgagattg and ctgagtatgtctgccctgtatgct; and 18S control, agtcctgccctttgtacaca and gatccgagggcctcactaaac, respectively.

Generation of NSMase-KD Cells Using siRNA. Two hairpin-forming oligonucleotides directed against NSMase mRNA were selected using the SiRNA design tool (http://bioinfo.clontech.com/rnaidesigner/frontpage.jsp) and cloned into RNAi-Ready pSIREN Retro-Q, according to the manufacturer's instructions. The two sequences were gatccGCAGGACTTCCAGTACTTAAAttcaagagatttaagtactggaagtcctgctttttg and gatccGCACGTCTATACTCTCAATGGttcaagagaccattgagagtatagacgtgctttttg, where the targeting sequences within the synthetic oligonucleotides are capitalized. Constructs that express the sRNAis were pSIREN-NSMase-1 and pSIREN-NSMase-2. Retroviruses were packaged in PT67 cells and used to infect INS-1 cells. A construct that encoded scrambled RNA was used to generate control cell lines. Cells were selected with 0.25 μg/mL puromycin, and single-cell clones were expanded. Total RNA was prepared from the various cell lines, and Northern blot analyses, as described previously (*75*), were performed to identify cell lines in which NSMase mRNA was knocked down. Cell lines of interest were selected for further expansion and study.

Statistical Analyses. Data were converted to means $\pm$ the standard error of the mean, and the Students' *t*-test was applied to determine significant differences between two samples ($p < 0.05$). Statistical differences between multiple treatment groups and a control group were determined using analysis of variances and the Dunnett post-hoc test.

RESULTS

Demonstration of iPLA$_2\beta$ Overexpression in INS-1 Cells. In this study, we examine the relationship among iPLA$_2\beta$, ceramides, and INS-1 cell apoptosis during ER stress. This was done in INS-1 insulinoma cells because they manifest endogenous iPLA$_2\beta$ activity analogous to that expressed in pancreatic islet β-cells, are susceptible to ER stress, provide an abundant source of starting material, and can be manipulated to over- or underexpress proteins of interest (*43*, *54*, *63*). To more directly examine the role of iPLA$_2\beta$ in ER stress-induced INS-1 cell apoptosis, parallel studies were done with iPLA$_2\beta$-overexpressing INS-1 cells (OE INS-1 cells). These cells, relative to empty vector-transfected INS-1 cells (V INS-1 cells), expressed higher levels of iPLA$_2\beta$ protein in the cytosol (Figure 1A, inset) and, as reported previously (*43*), a nearly 15-fold higher iPLA$_2\beta$ catalytic activity [V, 79 $\pm$ 8 pmol (mg of protein)$^{-1}$ min^{-1}; and OE, 1386 $\pm$ 434 pmol (mg of protein)$^{-1}$ min^{-1} ($n = 5$ in each group)]. As expected, iPLA$_2\beta$ catalytic activity manifested in the transfected INS-1 cells exhibited characteristic properties of the enzyme: stimulation by ATP [V, 272 $\pm$ 18 pmol (mg of protein)$^{-1}$ min^{-1}; and OE, 3688 $\pm$ 503 pmol (mg of protein)$^{-1}$ min^{-1}] and inhibition by BEL (residual activity near zero in both groups).

ER Stress-Induced INS-1 Cell Apoptosis Is Amplified in iPLA$_2\beta$-OE INS-1 Cells. In light of the earlier observation of a higher incidence of apoptosis of OE INS-1 cells (*63*), in this study, we examined whether progression of apoptosis due to thapsigargin-induced ER stress differed in V and OE INS-1 cells. Because the incidence of INS-1 cell apoptosis during the first 11 h was unchanged, only data from vehicle-treated and cells treated with thapsigargin for 12 and 24 h are presented. TUNEL staining analyses (Figure 1A) revealed that the abundance of TUNEL-positive INS-1 cells was minimal at 0 h and progressively increased following treatment with thapsigargin for 12 and 24 h in both V and

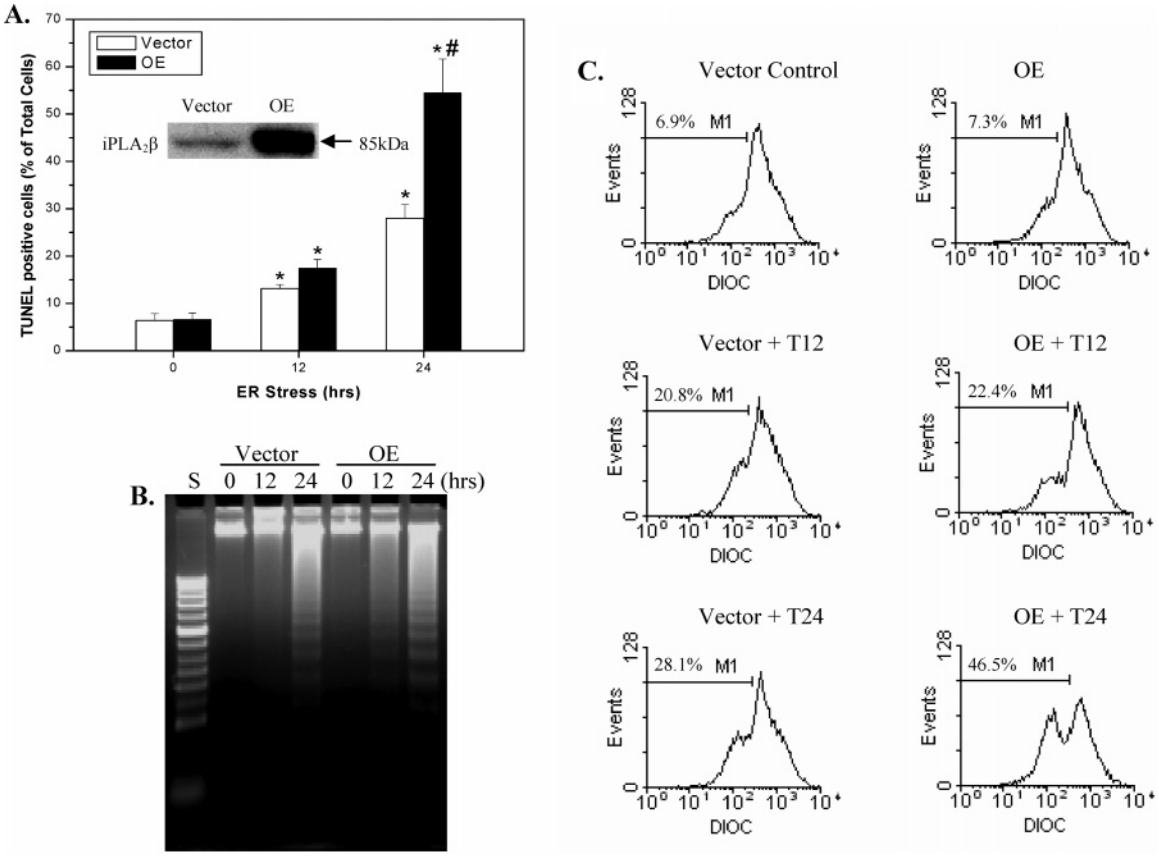

FIGURE 1: ER stress-induced apoptosis in INS-1 cells. INS-1 cells were treated with either vehicle (DMSO) or thapsigargin (T, 1 μM) and incubated at 37 °C under an atmosphere of 95% CO_2 and 5% O_2 for up to 24 h. The cells were collected at 0, 12, and 24 h to determine the incidence of apoptosis. (A) TUNEL-positive cells. Percentages of TUNEL-positive cells relative to the total number of cells (DAPI-stained) were determined in a minimum of six fields on each slide from each experiment. Data represent means ± SEM of values obtained from five to seven separate experiments. The inset shows iPLA$_2\beta$-immunoreactive protein. Asterisks indicate the treated groups are significantly different from corresponding 0 h control groups ($p < 0.05$). The number sign indicates the OE-treated group at 24 h is significantly different from all other groups ($p < 0.05$). (B) DNA laddering. (C) Mitochondrial membrane potential (MitoMP). Representative fluorescence spectra generated from analyses of 10 000 INS-1 cells from each experiment by flow cytometry are presented. M1 refers to the percentage of cells in which MitoMP is compromised (each assay was carried out three to five times).

OE INS-1 cells. The abundance of apoptotic cells in the OE group at 24 h, however, was 2-fold greater than in the V group.

As accurate quantitation of TUNEL-positive cells is not easily achieved, the incidence of apoptosis following induction of ER stress in the INS-1 cells with thapsigargin was assessed by two additional methods. In the DNA laddering assay shown in Figure 1B, DNA fragmentation, which occurs in cells undergoing apoptosis, was not detected in the V group at 12 h but was evident at 24 h. In contrast, DNA fragmentation in the OE group was detectable by 12 h and was more pronounced at 24 h than in the V group. The second assay measured loss of MitoMP, which is another hallmark of cellular apoptosis, in a suspension of cells to which a fluorescent MitoFlow reagent was added. This reagent concentrates in the mitochondria of healthy cells, but the mitochondria of cells undergoing apoptosis become compromised and accumulate less of the reagent; this is reflected by a decrease in the fluorescence signal and the appearance of a second peak that is left of the original. The spectra presented in Figure 1C reflect fluorescence measurement in 10 000 INS-1 cells, and the percentage of cells losing MitoMP, analyzed by the application software, is indicated as M1. As illustrated, there was a gradual appearance of a second peak over a 24 h period of ER stress, indicative of an increase in the number of INS-1 cells with compromised MitoMP. However, relative to the V group, a second peak begins to emerge in the OE group by 12 h, suggesting that the MitoMP is affected in a higher number of cells in this group by this time [V, 22.00 ± 0.01%; and OE, 25.04 ± 0.01% ($p = 0.004965$; $n = 5$ in each group)]. At 24 h, a greater percentage of OE INS-1 cells were seen to lose MitoMP, relative to the V INS-1 cells.

Thapsigargin Induces Expression of GRP78, CHOP, and PAPR in INS-1 Cells. To confirm induction of ER stress in INS-1 cells treated with thapsigargin, expression of ER stress factors GRP78 and CHOP was examined in cytosol prepared from vehicle- and thapsigargin-treated INS-1 cells. Immunoblotting analyses revealed induction of both within 2−4 h (Figure 2A). To quantify their expression levels, the density of GRP78 and CHOP immunoreactivity to the internal control tubulin immunoreactivity at corresponding times was determined. Representative analyses illustrated in panels B and C of Figure 2 indicated increases in the density of GRP78 between 2 and 4 h and in that of CHOP between 4 and 8 h. They further revealed that between 4 and 16 h, the level of expression of both was greater in the OE group than in the V group. A key protein that is selectively cleaved at the onset of apoptosis by caspases is poly(ADP-ribose) polymerase (PARP) (*76*). Cleavage of PARP leads to generation of an

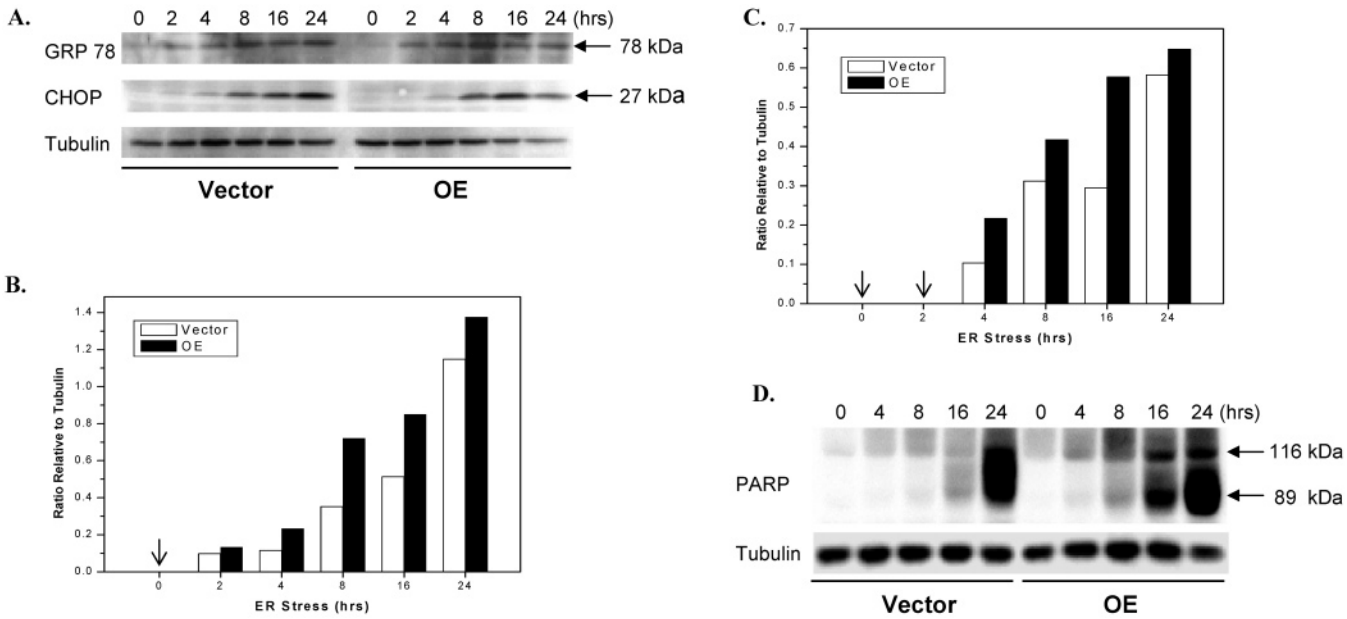

FIGURE 2: ER stress-induced expression of GRP78, CHOP, and PARP in INS-1 cells. INS-1 cells were treated with either vehicle (DMSO) or thapsigargin (T, 1 μM). At various times, the cells were harvested and cytosolic fractions prepared and processed for immunoblot analyses. (A) ER stress factors GRP78 and CHOP. (B and C) Densitometric analyses of GRP78 and CHOP expression, respectively, relative to internal control tubulin (arrows indicate nondetectable levels of expression). (D) PARP. Immunoreactive bands were visualized by enhanced chemiluminescence (each assay was carried out a minimum of three times).

active product that facilitates cellular disassembly (*77*). In both V and OE INS-1 cells, thapsigargin-induced ER stress resulted in cleavage of PARP (Figure 2D), but it occurred earlier and was more profound in the OE group than in the V group. Collectively, the data presented in Figures 1 and 2 reveal a sequence of thapsigargin-induced events that are characteristic of an ER stress response in INS-1 cells beginning with expression of GRP78 followed by CHOP, cleavage of PARP, and finally apoptotic cell death.

ER Stress Induces Increases in Neutral Sphingomyelinase Message Levels in INS-1 Cells, and This Is Inhibited by BEL. We previously reported temporal increases in the level of ceramide generation in INS-1 cells during a 24 h period following induction of ER stress (*63*). An increase in cellular ceramide levels can occur via *de novo* synthesis, sphingomyelin breakdown, or a decreased level of degradation of ceramides. To determine which pathway is prominent in INS-1 cells undergoing ER stress, total RNA was prepared from vehicle-treated and thapsigargin-treated INS-1 cells for quantitative PCR analyses of enzymes in each pathway: serine palmitoyltransferase (SPT), which catalyzes the rate-limiting step in the *de novo* pathway; neutral sphingomyelinase (NSMase), which catalyzes the hydrolysis of sphingomyelins; and ceramidase, which catalyzes the degradation of ceramides. As shown in Figure 3A, mRNA levels for SPT were not significantly altered while the level of ceramidase message expression decreases over the course of ER stress. In contrast, ER stress increased the level of NSMase mRNA expression in the INS-1 cells and its level of expression in the OE INS-1 cells was found to be more sensitive to ER stress, as reflected by the earlier onset of the increase in these cells relative to the V INS-1 cells (2 h vs 6 h). Additionally, steady-state levels of NSMase message reached between 12 and 16 h were 2-fold higher in the OE INS-1 cells than in the V INS-1 cells.

The increased sensitivity of NSMase expression to ER stress and the amplification of the increase in iPLA$_2\beta$-overexpressing INS-1 cells suggested that NSMase expression might be modulated by iPLA$_2\beta$. To test this possibility, ER stress was induced in OE INS-1 cells in the absence or presence of BEL. Twelve hours following the induction of ER stress, the cells were harvested for quantitative PCR analyses. As shown in Figure 3B, BEL not only reduced control levels of NSMase expression but almost completely prevented the induction of NSMase expression at 12 h. In contrast, ceramidase mRNA levels, which were decreased similarly in ER-stressed V and OE INS-1 cells, were not returned to basal levels by BEL. A small decrease in SPT mRNA levels was seen in control V INS-1 cells, but there was no significant effect of BEL in the ER-stressed INS-1 cells. These findings suggest that ER stress induces iPLA$_2\beta$-mediated expression of NSMase in INS-1 cells.

ER Stress Induces Increases in ER-Associated iPLA$_2\beta$ Protein and Catalytic Activity and Concomitant NSMase Protein Expression That Is Inhibited by Inactivation of iPLA$_2\beta$ with BEL. To further examine the link among ER stress, iPLA$_2\beta$ activation, and NSMase expression, the effects of ER stress on ER-associated iPLA$_2\beta$ were first examined. The ER fraction was prepared from V and OE INS-1 cells using an ER isolation kit, and organelle marker analyses verified that this fraction was enriched in ER protein calnexin, but not in proteins associated with other organelles (data not shown). As shown in Figure 4A, ER stress led to temporal accumulations of ER-associated iPLA$_2\beta$ protein between 2 and 8 h. This was reflected by increases in ER-associated iPLA$_2\beta$ catalytic activity (Figure 4B). Levels of both iPLA$_2\beta$ protein accumulation and catalytic activity in the ER during ER stress were greater in OE INS-1 cells than in V INS-1 cells.

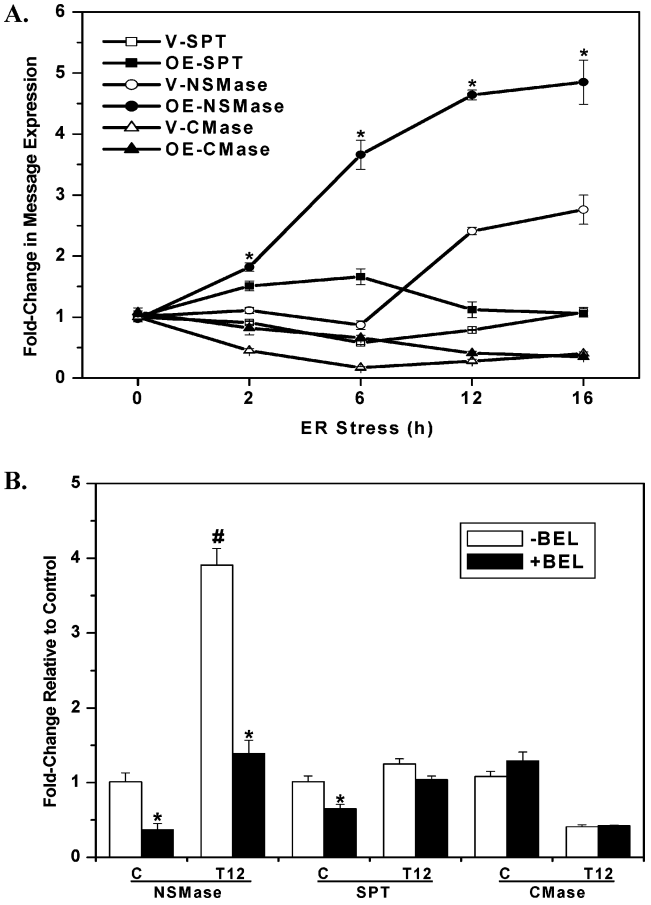

FIGURE 3: ER stress-induced expression of neutral sphingomyelinase (NSMase) message in INS-1 cells with or without BEL. INS-1 cells were treated with either vehicle (DMSO, C) or thapsigargin (T, 1 μM) and cultured for up to 16 h in the absence or presence of BEL (1 μM). Total RNA was prepared from the cells at various times for quantitative (Q) RT-PCR analyses for enzymes that participate in the generation of ceramides via the *de novo* pathway: serine palmitoyltransferase (SPT), sphingomyelin hydrolysis (NSMase), and inhibition of ceramide degradation (CMase, ceramidase). (A) QRT-PCR analyses of SPT, NSMase, and CMase ($n = 4$). Asterisks indicate the OE NSMase group is significantly different from the V NSMase group ($p < 0.05$). (B) QRT-PCR analyses of NSMase, SPT, and ceramidase with or without BEL in control cells and 12 h after induction of ER stress (T12) ($n = 4$). Asterisks indicate the BEL-treated group is significantly different from the corresponding untreated group ($p < 0.05$). The number sign indicates the untreated NSMase group at 12 h is significantly different from other NSMase groups ($p < 0.05$).

We next examined whether induction of NSMase message during ER stress leads to an increased level of expression of NSMase protein and whether this could be inhibited by inactivation of iPLA$_2\beta$. As seen in Figure 4C, a temporal increase in the level of NSMase protein expression is seen in ER-stressed INS-1 cells, with the increases being greater in the OE INS-1 cells. Pretreatment of the INS-1 cells with BEL for 1 h prior to induction of ER stress resulted in inhibition of induction of NSMase protein for up to 16 h. During this period, iPLA$_2\beta$ catalytic activity was inhibited in the V INS-1 cells by 95, 78, 83, and 78% and by 97, 90, 79, and 58% in the OE INS-1 cells at 0, 4, 8, and 16 h, respectively. These findings support and strengthen an association between NSMase expression and iPLA$_2\beta$ activation in ER-stressed INS-1 cells.

ER Stress Induces Decreases in the Relative Abundances of Sphingomyelin Molecular Species in INS-1 Cells. To allow quantitation of INS-1 cell sphingomyelins, standard curves for various molecular species were first constructed. Because commercially available synthetic sphingomyelins were not available when these studies were initiated, natural sphingomyelins from egg and brain (Avanti Polar Lipids) were used. To identify the individual species, the amounts of the natural sphingomyelins were varied in the presence of a constant amount of an internal standard and ESI-MS/MS with constant neutral loss scanning of 59 [$[M + Li]^+ - N(CH_3)_3$] was performed. 14:0/14:0-Glycero-phosphocholine (GPC, *m*/*z* 684) was used as the internal standard because it does not occur naturally in rats, mice, humans, or INS-1 cells. Next, the sphingomyelins were saponified to liberate the individual fatty acids and their ratios determined using d_8-arachidonic acid as an internal standard. The percent contribution of individual fatty acids to the total fatty acid content of each source was then determined and used to construct standard curves of the individual sphingomyelin species (Figure 5).

To determine whether induction of NSMase mRNA during ER stress is associated with an increased level of sphingomyelin hydrolysis, lipid extracts were prepared in the presence of the 14:0/14:0-GPC internal standard from vehicle-treated and ER-stressed INS-1 cells and analyzed by ESI-MS/MS. As shown in Figure 6A (inset), the prominent ions in the total ion current spectrum of GPC are those of the even mass PC species. The emergence of the odd *m*/*z* sphingomyelin species is facilitated by constant neutral loss of 59 (Figure 6A). Figure 6 displays the positive ion ESI-MS TIC tracing of Li^+ adducts of the sphingomyelin species in INS-1 cell lipids after addition of the 14:0/14:0-GPC internal standard, which is represented in the spectrum by its $[M + Li]^+$ ion (*m*/*z* 684). As with the ceramide species, the major sphingomyelin species endogenous to INS-1 cells are 16:0 (*m*/*z* 709), 18:0 (*m*/*z* 737), 22:0 (*m*/*z* 793), 24:1 (*m*/*z* 819), and 24:0 (*m*/*z* 821). The spectra were acquired by monitoring constant neutral loss of 59 in V and OE INS-1 cells treated with either vehicle (Figure 6A,C) or thapsigargin (Figure 6B,D). Following induction of ER stress, the relative abundances of the sphingomyelins in both V (Figure 6B) and OE (Figure 6D) INS-1 cells decreased, which is reflected by the decreases in the intensities of ions representing them.

ER Stress-Induced Generation of Ceramides and Sphingomyelin Hydrolysis in INS-1 Cells Are Inhibited by BEL. To examine whether iPLA$_2\beta$ participates in ceramide generation or sphingomyelin hydrolysis in ER-stressed INS-1 cells, the cells were treated with thapsigargin in the absence or presence of BEL, a suicide inhibitor of iPLA$_2\beta$. In the absence of ER stress, the total ceramide pool in INS-1 cells was found to be similar (V, 8.37 $\pm$ 2.01 nmol/μmol of PO_4; and OE, 8.18 $\pm$ 2.17 nmol/μmol of PO_4). ER stress induced an increase in all of the identified ceramide species in both V and OE INS-1 cells (Table 1), and the increase in the total ceramide pool was 2-fold higher in the OE cells than in the V INS-1 cells (Figure 7A). BEL alone had no effect in the absence of ER stress (data were therefore combined with corresponding control groups), but addition of BEL to ER-stressed cells resulted in inhibition of ceramide generation.

In the absence of ER stress, the total sphingomyelin pools in the V and OE INS-1 cells were also not found to be different (V, 118 $\pm$ 14 pmol/μmol of PO_4; and OE, 111 $\pm$ 12 pmol/μmol of PO_4). Quantitation of individual sphingo-

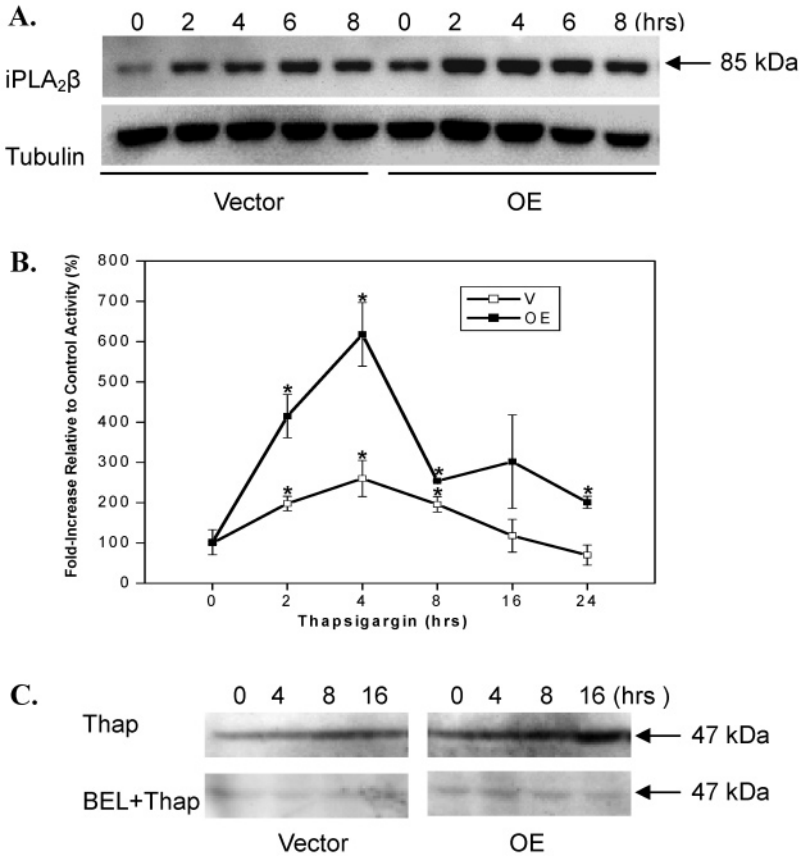

FIGURE 4: Effects of ER stress on ER-associated iPLA$_2\beta$ and on NSMase protein with or without BEL in INS-1 cells. ER fractions were prepared from control and thapsigargin-treated V and OE INS-1 cells to determine ER-associated (A) iPLA$_2\beta$ protein expression and (B) catalytic activity. Asterisks indicate the activity is significantly different from those of corresponding untreated basal controls ($p < 0.05$; $n = 5-9$). (C) INS-1 cells were treated without or with BEL (10 μM) for 1 h prior to vehicle or thapsigargin (1 μM) exposure, and NSMase protein expression in homogenates was examined via immunoblot analyses.

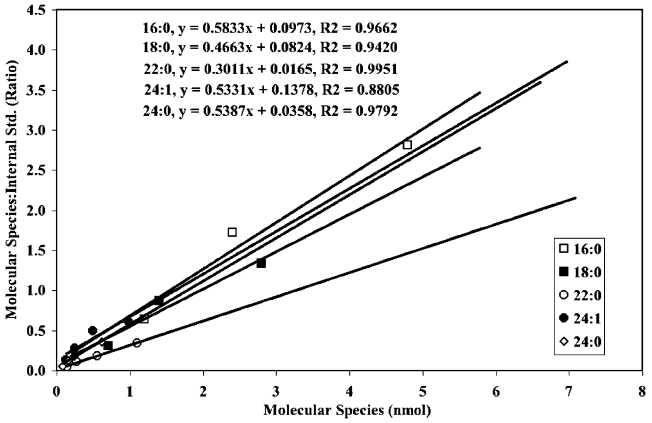

FIGURE 5: Standard curves for sphingomyelin molecular species. Commercially available synthetic sphingomyelins from egg and brain were used to construct standard curves in the presence of a (14:0/14:0)-GPC internal standard (IS, *m*/*z* 684), as described in the Results. The internal standard concentration was kept constant while the concentration of the sphingomyelins was varied.

myelin species revealed decreases in the levels of major endogenous sphingomyelin species in both V and OE INS-1 cells subjected to ER stress, reflecting an increase in the extent of sphingomyelin hydrolysis (Table 2), and as shown in Figure 7B, ER stress induced a 2-fold greater decrease in the total sphingomyelin pool in the OE group, in comparison with the V group. Addition of BEL resulted in prevention of ER stress-induced decreases in the extent of sphingomyelin hydrolysis in both V and OE INS-1 cells. The data presented in Tables 1 and 2 and Figures 3−7 therefore suggest that ER stress induces NSMase expression in INS-1 cells, leading to hydrolysis of sphingomyelins and generation of ceramides, and that iPLA$_2\beta$ participates in this process.

ER Stress-Induced Ceramide Generation, Sphingomyelin Hydrolysis, and INS-1 Cell Apoptosis Are Suppressed by Inhibition of NSMase but Not the de Novo Synthesis Pathway. We next examined whether sphingomyelin hydrolysis or the de novo synthesis pathway is the more important contributor to the generation of ceramides in ER-stressed INS-1 cells. Lipids were extracted from INS-1 cells treated with either vehicle or thapsigargin in the absence or presence of either the SPT inhibitor L-cycloserine (LCS) or the NSMase inhibitor GW4869 (GW). These inhibitors and the concentrations of the inhibitors used in this study have been widely used to distinguish ceramide-generating pathways in various cell systems, including pancreatic islets (*78*, *79*). ESI-MS/MS analyses used to determine the ceramide and sphingomyelin contents revealed the lack of an effect of inhibitor treatment alone (data were therefore combined with corresponding controls). LCS also failed to prevent ER stress-induced changes in ceramides or sphingomyelins (Tables 1 and 2 and Figure 8A,B). In contrast, GW4869 suppressed both the increase in the extent of ceramide generation and decrease in the level of sphingomyelins in the ER-stressed INS-1 cells. These data taken together with the finding of an increased level of NSMase, but not SPT, message expression suggest that ER stress-induced ceramide genera-

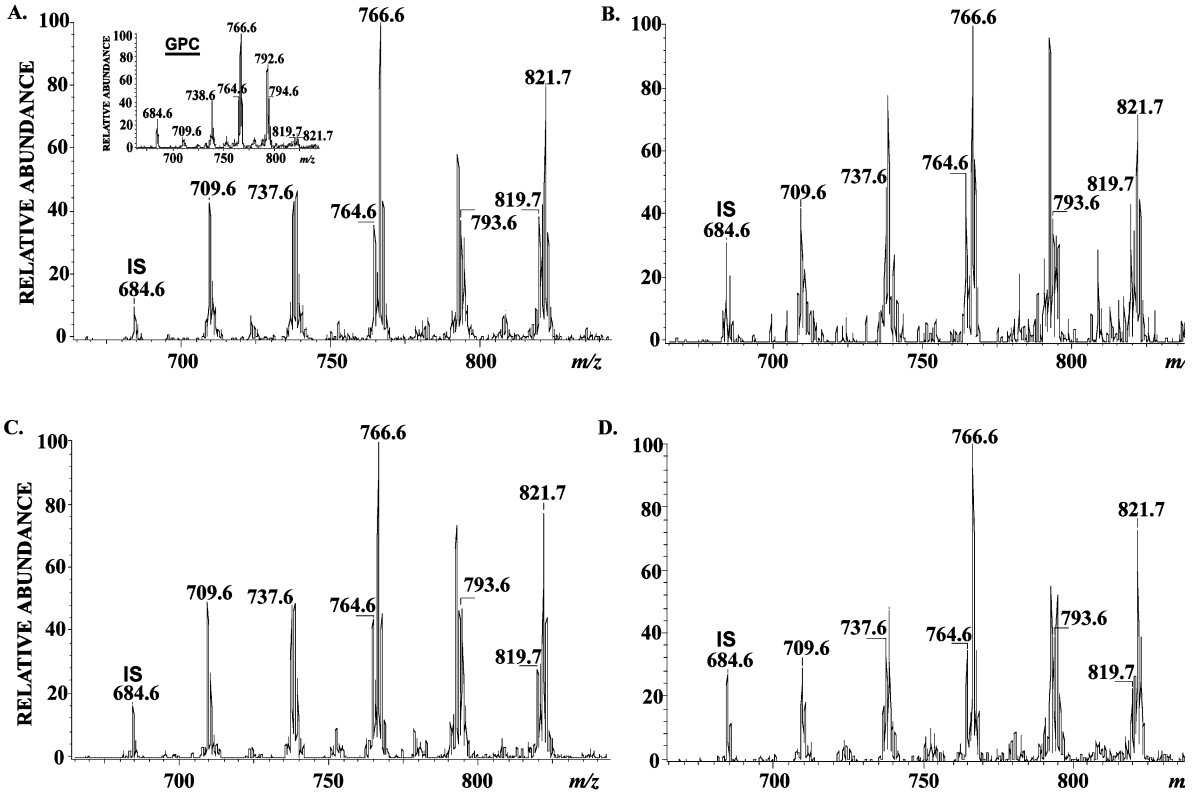

FIGURE 6: INS-1 cell sphingomyelin analyses by electrospray (ESI) ionization mass spectrometry. INS-1 cells were treated with either vehicle (DMSO, control) or thapsigargin (T, 1 μM) for 24 h. The cells were detached and washed in phosphate-buffered saline; extraction buffer containing (14:0/14:0)-glycero-phosphocholine (GPC) internal standard (IS, *m*/*z* 684) was added to the cells, and lipids were extracted under acidic conditions. Relative abundances of sphingomyelin (SM) molecular species were analyzed by ESI-MS/MS by monitoring constant neutral loss scanning of 59: (A) vector control (inset, total ion current of GPC), (B) vector with T, (C) OE control, and (D) OE with T. The major sphingomyelin molecular species are indicated in each spectrum: 16:0 (*m*/*z* 709), 18:0 (*m*/*z* 737), 22:0 (*m*/*z* 793). 24:1 (*m*/*z* 819), and 24:0 (*m*/*z* 821).

Table 1: Thapsigargin-Induced Changes in Ceramide Molecular Species in Vector (V) and iPLA$_2\beta$-Overexpressing (OE) INS-1 Cells in the Absence and Presence of Inhibitors[a]

	C:DB	VC	VT	V + BEL	V + GW	V + LCS	OEC	OET	OE + BEL	OE + GW	OE + LCS
m/*z* 544	16:0	100 ± 11	196 ± 27	35 ± 10	157 ± 28	458 ± 74	100 ± 8	340 ± 57	116 ± 46	258 ± 37	560 ± 78
m/*z* 572	18:0	100 ± 13	194 ± 24	48 ± 9	146 ± 21	335 ± 138	96 ± 12	379 ± 92	140 ± 65	248 ± 28	742 ± 203
m/*z* 628	22:0	100 ± 20	280 ± 106	58 ± 5	99 ± 16	771 ± 0	98 ± 13	670 ± 268	228 ± 47	310 ± 106	1423 ± 363
m/*z* 654	24:1	100 ± 13	168 ± 20	53 ± 12	114 ± 20	402 ± 54	99 ± 8	401 ± 119	166 ± 48	299 ± 89	741 ± 7
m/*z* 656	24:0	100 ± 12	200 ± 24	53 ± 9	121 ± 16	405 ± 88	102 ± 6	305 ± 67	146 ± 77	195 ± 29	542 ± 150

[a] Lipids were extracted from V and OE INS-1 cells, and ceramides were analyzed by ESI-MS/MS and quantitated. Thapsigargin-induced changes in individual ceramide molecular species in the absence and presence of inhibitors of iPLA$_2\beta$ (BEL, 10 μM), SPT (LCS, 1 μM), or NSMase (GW, 10 μM), relative to corresponding controls, are presented as means ± SEM.

tion in INS-1 cells most likely occurs via an increased level of hydrolysis of sphingomyelins.

As *de novo* synthesis of ceramides was reported to participate in lipoapoptosis of β-cells (*79*), the possibility that this pathway may also contribute to ER stress-induced INS-1 cell apoptosis was examined. As reflected by DNA laddering and MitoMP analyses (panels C and D of Figure 8, respectively), treatment with the inhibitor alone had no effect and LCS was unable to prevent ER stress-induced INS-1 cell apoptosis. In contrast, inhibition of NSMase prevented DNA fragmentation and significantly suppressed the compromising of MitoMP in ER-stressed INS-1 cells. Collectively, these findings suggest that NSMase-mediated increases in the extent of ceramide generation, but not *de novo* synthesis of ceramides, contribute to ER stress-mediated INS-1 cell apoptosis.

Knockdown (KD) of NSMase Suppresses ER Stress-Induced Ceramide Generation, Sphingomyelin Hydrolysis, and INS-1 Cell Apoptosis. To further establish the relationship between ER stress, iPLA$_2\beta$, NSMase, and INS-1 cell apoptosis, we used sRNAi technology to generate INS-1 cells in which NSMase is knocked down (KD). This protocol resulted in the identification by Northern analyses of V and OE INS-1 cell lines in which NSMase was knocked down. One OE cell line (OE KD3) in which sRNAi treatment failed to suppress NSMase message was included as a negative control. As illustrated in Figure 9A, NSMase KD completely prevented induction of NSMase message in ER-stressed INS-1 cells. As expected, induction of NSMase was not suppressed in the OE KD3 cells.

We next determined whether knockdown of NSMase is able to suppress ER stress-induced affects on ceramides, sphingomyelins, and INS-1 cell apoptosis. Levels of ceramides and sphingomyelins in untreated control (V and OE INS-1 cells infected with construct encoded with scrambled RNA) and NSMase KD V and OE INS-1 cells were found

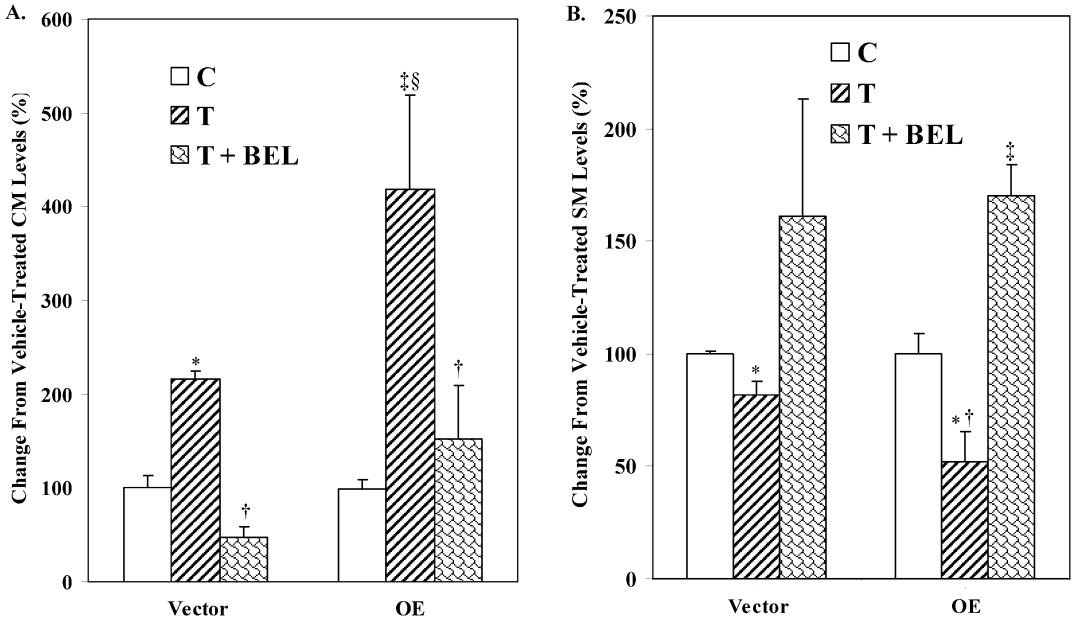

FIGURE 7: ER stress-induced ceramide generation and sphingomyelin hydrolysis in INS-1 cells are inhibited by BEL. Following MS analyses, the ratios of each ceramide and sphingomyelin molecular species, relative to the internal standard, were determined. The individual molecular species (16:0, 18:0, 22:0. 24:1, and 24:0) were then normalized to total lipid phosphorus content, and the changes in total ceramide and sphingomyelin pools, relative to ceramide and sphingomyelin pools in untreated control cells, are presented as means ± SEM ($n = 7-9$). BEL treatment alone had no significant effect, and the data were combined with those from corresponding vehicle-treated groups. (A) Total ceramides. A double dagger and a section mark together indicate the treated groups are significantly different from corresponding control groups at $p < 0.005$ and 0.0005, respectively. Daggers indicate that the BEL-treated groups are significantly different from corresponding treated groups ($p < 0.05$). The asterisk indicates the OET group is significantly different from the VT group ($p < 0.05$). (B) Total sphingomyelins. Asterisks indicate the treated groups are significantly different from corresponding control groups ($p < 0.01$). The dagger indicates the OET group is significantly different from the VT group ($p < 0.05$). The double dagger indicates the BEL-treated groups are significantly different from corresponding control and treated groups ($p < 0.05$).

Table 2: Thapsigargin-Induced Changes in Sphingomyelin Molecular Species in Vector (V) and iPLA$_2\beta$-Overexpressing (OE) INS-1 Cells in the Absence and Presence of Inhibitors[a]

	C:DB	VC	VT	V + BEL	V + GW	V + LCS	OEC	OET	OE + BEL	OE + GW	OE + LCS
m/z 709	16:0	100 ± 5	81 ± 9	163 ± 58	129 ± 38	43 ± 21	100 ± 11	59 ± 18	227 ± 49	145 ± 11	34 ± 14
m/z 737	18:0	100 ± 5	86 ± 11	180 ± 68	109 ± 12	35 ± 30	100 ± 10	52 ± 18	166 ± 20	119 ± 9	31 ± 2
m/z 793	22:0	100 ± 3	78 ± 12	147 ± 63	147 ± 27	41 ± 35	100 ± 10	45 ± 12	158 ± 10	174 ± 39	31 ± 17
m/z 819	24:1	100 ± 3	75 ± 7	160 ± 39	130 ± 26	76 ± 13	100 ± 15	55 ± 16	187 ± 18	161 ± 28	125 ± 20
m/z 821	24:0	100 ± 4	88 ± 13	161 ± 57	130 ± 26	81 ± 17	100 ± 5	75 ± 19	179 ± 5	192 ± 18	103 ± 11

[a] Lipids were extracted from V and OE INS-1 cells, and sphingomyelins were analyzed by ESI-MS/MS and quantitated. Thapsigargin-induced changes in individual sphingomyelin molecular species in the absence and presence of inhibitors of iPLA$_2\beta$ (BEL, 10 μM), SPT (LCS, 1 μM), or NSMase (GW, 10 μM), relative to corresponding controls, are presented as means ± SEM.

to be similar and pooled separately and presented as "V C" and "OE C" bars. As the data in thapsigargin-treated V KD and OE KD1 and KD2 INS-1 cells were similar, they were pooled and presented as a single "KDT" bar. Similarly, as the data obtained for thapsigargin-treated OE KD3 cells were similar to those for thapsigargin-treated OE INS-1 cells, they were pooled and presented as a single "OE T" bar. As illustrated in Figure 9, NSMase KD completely abolished ER stress-induced increases in the level of ceramide generation (Figure 9B) and sphingomyelin hydrolysis (Figure 9C) in ER-stressed INS-1 cells. DNA laddering analyses (Figure 9D) revealed that ER stress induced with thapsigargin promoted DNA fragmentation in the V, OE, and OE KD3 INS-1 cells, but not in the V KD or OE KD INS-1 cells. The findings further support the involvement of NSMase in ER stress-induced INS-1 cell apoptosis.

DISCUSSION

It is becoming widely accepted that apoptosis plays a prominent role in the loss of β-cells during the progression of diabetes mellitus (*2*, *10*, *11*, *14*, *16*−*20*, *80*−*82*). It is therefore important to gain a better understanding of the processes that lead to apoptotic β-cell death so that more targeted therapeutic measures can be used to prevent or delay this process. Among the recognized apoptotic signaling pathways (*22*, *23*), β-cell death in the Akita diabetic (*15*, *21*) and NOD.k iHEL nonimmune (*83*) diabetic mouse models have been reported to be due to ER stress. Wolfram syndrome, which is associated with juvenile-onset diabetes mellitus, is also thought to be a consequence of chronic ER stress in pancreatic β-cells (*80*−*82*). These reports raise the possibility that the ER stress pathway contributes to β-cell losses in diabetes. However, very little is currently known about the cellular events that are triggered by ER stress and that eventually lead to β-cell apoptosis. As such, elucidation of the mechanisms that contribute to ER stress-induced β-cell apoptosis is very much warranted.

Earlier findings in insulinoma cells (*39*) and pancreatic islets (*40*) using inhibitors of SERCA to deplete ER Ca^{2+} stores (*38*) suggested that the group VIA Ca^{2+}-independent

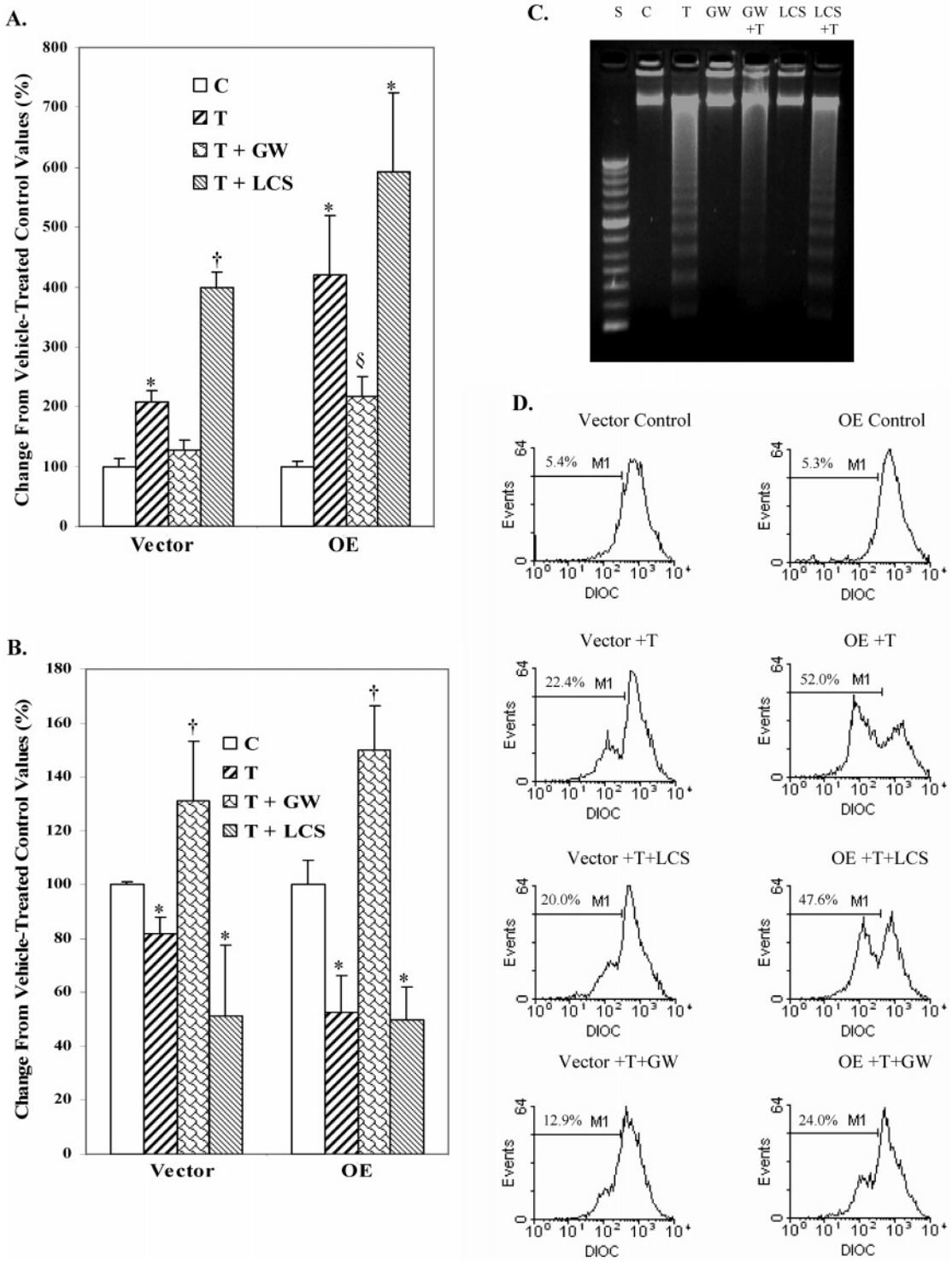

FIGURE 8: Effects of NSMase and SPT inhibition on ER stress-induced ceramide generation, sphingomyelin hydrolysis, and INS-1 cell apoptosis. INS-1 cells were treated with either vehicle (C) or thapsigargin (T, 1 μM) and cultured for up to 24 h in the absence or presence of the NSMase inhibitor GW4869 (GW, 10 μM) or the SPT inhibitor L-cycloserine (LCS, 1 mM). At various times, cells were detached and processed for ceramide, sphingomyelin, and apoptosis analyses. The relative abundances of individual ceramide and sphingomyelin molecular species were analyzed by ESI-MS/MS and quantitated relative to lipid phosphorus. The data are presented as means ± SEM ($n = 3-4$ in each group) of change in total ceramides and sphingomyelins, relative to untreated control groups. (A) Total ceramides. Asterisks indicate the treated groups are significantly different from corresponding control (C) groups ($p < 0.005$). The dagger indicates the VT and LCS group is significantly different from other vector groups ($p < 0.0001$). The section mark indicates the OET and GW group is significantly different from other OE groups ($p < 0.05$). (B) Total sphingomyelins. Asterisks indicate the groups that are significantly different from corresponding control (C) groups ($p < 0.05$). Daggers indicate the T and GW groups are significantly different from corresponding control (C) groups ($p < 0.01$). (C) DNA laddering. (D) MitoMP.

PLA_2 ($iPLA_2\beta$) participates in ER stress-induced β-cell apoptosis. We have since demonstrated that ER stress induces apoptosis of INS-1 insulinoma cells and that the incidence of apoptosis (a) is inhibited by BEL, a suicide-inhibitor of $iPLA_2\beta$, (b) is amplified in OE INS-1 cells, and (c) correlates with the expression levels of $iPLA_2\beta$ protein and activity (*63*). These findings are consistent with a role for $iPLA_2\beta$ in ER stress-induced β-cell apoptosis.

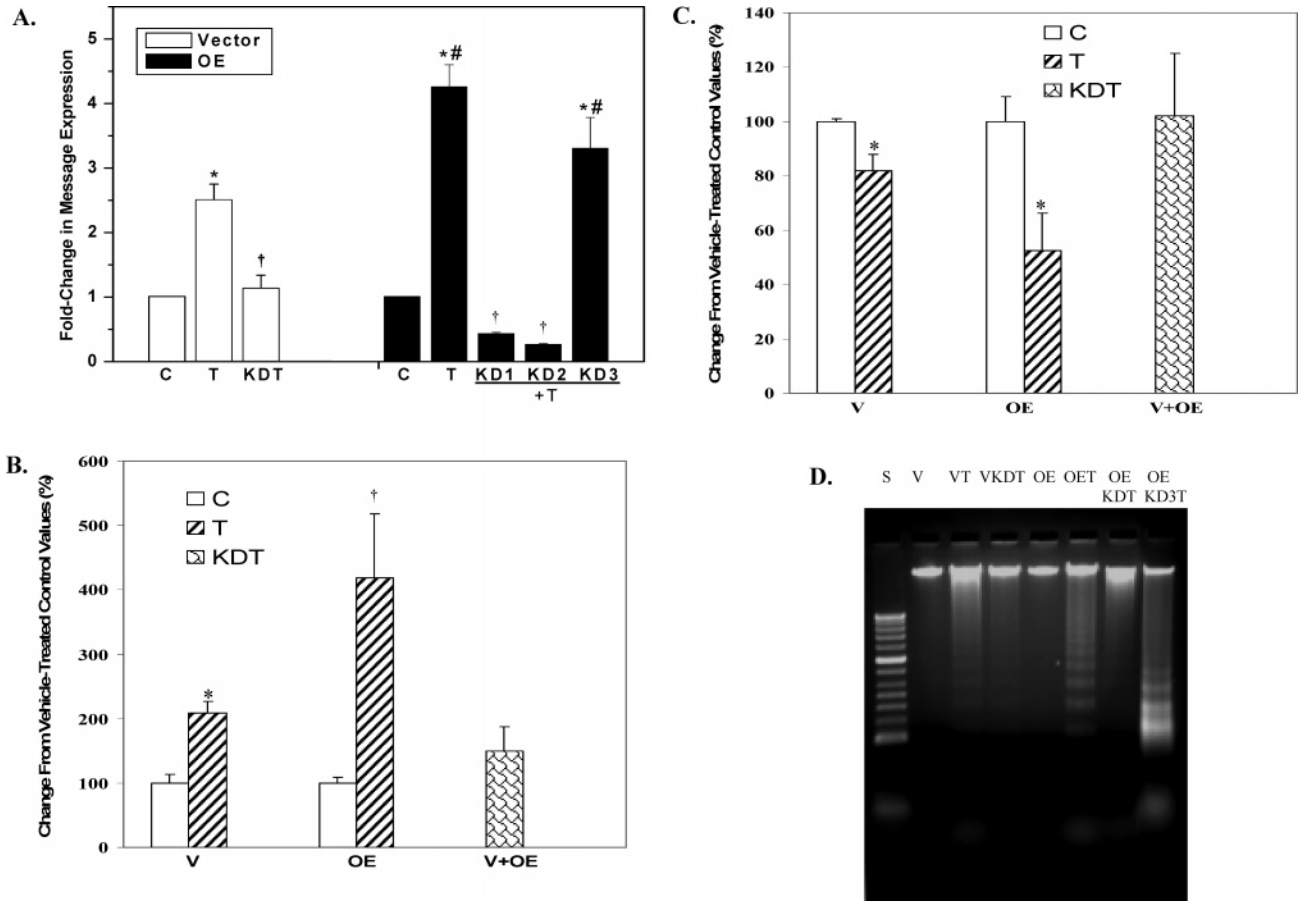

FIGURE 9: Effects of NSMase knockdown on ER stress-induced ceramide generation, sphingomyelin hydrolysis, and INS-1 cell apoptosis. sRNAi was used to knock down NSMase in the INS-1 cells. Single-cell clones were then cultured to confluency, and total RNA was isolated to determine the level of expression of NSMase message. Selected cell lines were then chosen for further study. (A) Effects of ER stress on NSMase expression in NSMase KD INS-1 cells. Parental INS-1 cells and INS-1 cells in which NSMase was knocked down were treated with either vehicle (DMSO, C) or thapsigargin (T, 1 μM). The cells were harvested at 16 h, and total RNA was prepared for QRT-PCR. The data are expressed as mean fold change $\pm$ SEM, relative to control ($n = 4-6$). Asterisks indicate the treated groups are significantly different from corresponding control groups ($p < 0.05$). Daggers indicate the KDT groups are significantly different from treated groups ($p < 0.05$). Number signs indicate the OE-treated groups are significantly different from other OE groups ($p < 0.05$). The relative abundances of individual ceramide and sphingomyelin molecular species were analyzed by ESI-MS/MS and quantitated relative to lipid phosphorus. The data are presented as means $\pm$ SEM ($n = 3-4$ in each group) of the change in total ceramides and sphingomyelins, relative to untreated control groups. As similar results were obtained in vehicle-treated V and V KD INS-1 cells and OE and OE KD INS-1 cells, they were pooled into two separate control values and presented as V C and OE C bars, respectively. The measurements in thapsigargin-treated V KD and OE KD cells were also found to be similar, and therefore, a combined value is presented as a single KDT bar. (B) Total ceramides. The asterisk indicates the VT group is significantly different from the corresponding control group ($p < 0.0005$). The dagger indicates the OET group is significantly different from all groups ($p < 0.005$). (C) Total sphingomyelins. Asterisks indicate the treated groups are significantly different from corresponding control (C) groups ($p < 0.01$). (D) DNA laddering.

A puzzling finding in that study was that ER stress also induced ceramide generation in INS-1. Further, the ceramides reached higher levels in iPLA$_2\beta$-overexpressing INS-1 cells, suggesting that iPLA$_2\beta$ might mediate ceramide generation in INS-1 cells during ER stress. Accumulations of cellular ceramides can be achieved by an increase in the extent of *de novo* synthesis from palmitate and other precursors (*79*) or hydrolysis of sphingomyelins, resulting in the generation of ceramide and phosphocholine (*84*), or by a decrease in the extent of degradation of ceramide (*85*, *86*). The *de novo* pathway is thought to participate in lipoapoptosis of β-cells (*79*, *86*), but as yet, there are no studies which examined ceramide generation during ER stress. In view of our earlier findings, it was therefore of interest to determine (a) which ceramide-generating pathway contributes to ceramide generation in ER-stressed INS-1 cells, (b) if iPLA$_2\beta$ is a requisite, and (c) whether inhibition of this pathway prevents ER stress-induced INS-1 cell apoptosis.

As in the earlier study (*63*), thapsigargin triggered an ER stress response (*15*, *35*, *36*), induced apoptosis, and increased the level of ceramide accumulation in INS-1 cells in this study. To examine whether INS-1 cell accumulations in ceramides during ER stress require iPLA$_2\beta$, ER stress was induced in INS-1 cells in the absence or presence of BEL and lipids were extracted for ESI-MS/MS analyses of ceramides (*73*). Such analyses revealed five major ceramide species that are endogenous to the INS-1 cells, and levels of nearly all of the ceramide species were increased in ER-stressed INS-1 cells. Inhibition of iPLA$_2\beta$ with BEL, however, completely prevented the increase in the total ceramide pool. These findings were taken to indicate that iPLA$_2\beta$ contributes to the increase in the level of ceramides in INS-1 cells during ER stress.

As the level of ceramide formation can be increased by different pathways, quantitative PCR analyses were used to examine message levels of ceramide-generating enzymes to

determine the source of the ceramide increases in INS-1 cells during ER stress. They included serine palmitoyltransferase (SPT), which catalyzes the rate-limiting step in de novo synthesis of ceramides (*79*); neutral sphingomyelinase (NSMase), which hydrolyzes sphingomyelins to generate ceramides and phosphocholine (*84*); and the ceramide-degrading enzyme ceramidase, inactivation of which by nitric oxide could lead to ceramide accumulations (*85*).

Unexpectedly, ER stress did not induce SPT message expression but increased NSMase mRNA and protein levels in the INS-1 cells. This is in contrast to earlier reports that de novo synthesis of ceramides contributes to lipoapoptosis of β-cells in ZDF rats (*79*) and of pancreatic islets exposed to free fatty acids (*86*, *87*). The increases in NSMase levels seen in our studies were accompanied by increases in the level of sphingomyelin hydrolysis, as reflected by decreases in the levels of sphingomyelin molecular species, identified by ESI-MS/MS analyses (*74*). Analogous to the effects of BEL on ceramide increases, both the increases in the levels of NSMase message and protein expression and sphingomyelin hydrolysis in ER-stressed INS-1 cells were inhibited by BEL. Further, chemical inhibition of NSMase activity or knockdown of NSMase not only was effective in preventing ceramide generation and sphingomyelin hydrolysis in ER-stressed INS-1 cells but also suppressed ER stress-induced INS-1 cell apoptosis. In contrast, inhibition of the *de novo* pathway was ineffective in preventing these consequences of ER stress in INS-1 cells. The ER stress pathway and the consequences of its induction that included increases in the level of ceramide generation, NSMase, sphingomyelin hydrolysis, and apoptosis were all accelerated and/or amplified in iPLA$_2\beta$-overexpressing (OE) INS-1 cells. As in the V INS-1 cells, inhibition of iPLA$_2\beta$ or NSMase was effective in preventing these ER stress-induced effects in the OE INS-1 cells, but inhibition of the *de novo* pathway was not. An alternate salvage pathway in which sphingoid bases generated by hydrolysis of complex sphingolipids by ceramidase are recycled into ceramides has recently been reported to also increase the level of ceramide formation (*88*). While this pathway was not examined directly in this study, the findings that ER stress did not increase mRNA levels of either ceramidase or iNOS (data not presented) might be taken to mean that the salvage pathway is most likely not a major pathway during ER stress in INS-1 cells. In fact, mRNA levels for ceramidase were modestly decreased by ER stress, and they remained unaffected by inhibition of iPLA$_2\beta$ with BEL. Our data therefore suggest that ceramides generated via hydrolysis of sphingomyelins by NSMase contribute to ER stress-induced INS-1 cell apoptosis and strongly support a role for iPLA$_2\beta$ in activation of this pathway.

While further studies are needed to elucidate the process by which ER stress affects iPLA$_2\beta$ and iPLA$_2\beta$ induces NSMase expression, a potential mechanism might be gleaned by considering these findings along with our earlier observations (*63*). In that study, ER stress was shown to stimulate iPLA$_2\beta$ activity and its perinuclear localization in INS-1 cells. As membranes of the nucleus and ER are contiguous (*89*, *90*), perinuclear accumulation of iPLA$_2\beta$ is consistent with association of the iPLA$_2\beta$ protein with a subcellular compartment that is likely to include ER (*89*). That this in fact is occurring is supported by our observation of increases in ER-associated iPLA$_2\beta$ protein and catalytic activity in the ER-stressed INS-1 cells. The ER in β-cells is enriched in arachidonate-containing phospholipids (*91*), and the increases in the level of iPLA$_2\beta$ protein would amplify the hydrolysis and subsequent metabolism of arachidonic acid. It is not unlikely that arachidonic acid and/or its bioactive metabolites (eicosanoids) stimulate the activity of NSMase in β-cells, as they do in other cell types (*92*−*96*), especially since there is evidence of NSMase in both nuclei and ER (*97*, *98*). Alternatively, arachidonic acid or eicosanoids, by virtue of their ability to regulate transcription of several gene families (*99*), could induce NSMase expression. This possibility is supported by these findings that inactivation of iPLA$_2\beta$ by BEL also inhibits NSMase message and protein expression and that NSMase KD INS-1 cells are resistant to ER stress-induced ceramide accumulation and apoptosis. These findings taken together with earlier demonstrations of inhibition of AA hydrolysis and eicosanoid generation in β-cells and INS-1 cells by BEL (*54*, *55*, *61*, *62*, *91*, *100*) strengthen the possibility that ER stress activates iPLA$_2\beta$, leading to the induction of NSmase and an increased level of generation of ceramides via this pathway. The various proposed roles of ceramides in cellular processes only increase the complexity of the potential mechanism(s) by which they could promote β-cell death during ER stress. It remains to be determined whether one molecular species of ceramide is more active and essential than another or whether an increase in the level of ceramides or a decrease in the level of sphingomyelins (*101*) is a more important factor in promoting β-cell death.

In summary, our findings demonstrate for the first time a link among ER stress-induced INS-1 insulinoma cell apoptosis, NSMase-mediated generation of ceramides, and iPLA$_2\beta$ activation. Our observations therefore increase the importance of gaining a better understanding of the role of iPLA$_2\beta$, not only in ER stress-mediated effects but also its potential role in β-cell apoptosis, a process that is gaining recognition as a major contributor to β-cell losses during the progression of diabetes.

ACKNOWLEDGMENT

We thank the expert technical assistance of Mr. Wu Jin, Dr. Mary Wohltmann, and Ms. Min Tan.

REFERENCES

1. Tisch, R., and McDevitt, H. (1996) Insulin-dependent diabetes mellitus, *Cell 85*, 291−297.
2. Mathis, D., Vence, L., and Benoist, C. (2001) β-Cell death during progression to diabetes, *Nature 414*, 792−798.
3. DeFronzo, R. A. (1988) Lilly lecture 1987. The triumvirate: β-cell, muscle, liver. A collusion responsible for NIDDM, *Diabetes 37*, 667−687.
4. DeFronzo, R. A. (1997) Insulin resistance: A multifaceted syndrome responsible for NIDDM, obesity, hypertension, dyslipidaemia and atherosclerosis, *Neth. J. Med. 50*, 191−197.
5. Kahn, C. R. (1995) Diabetes. Causes of insulin resistance, *Nature 373*, 384−385.
6. Kudva, Y. C., and Butler, P. C. (1997) Insulin secretion in type 2 diabetes mellitus, in *Clinicl Research in Diabetes and Obesity* (Draznin, B., and Rizza, R., Eds.) pp 119−136, Humana Press, Totowa, NJ.
7. Clark, A., Wells, C. A., Buley, I. D., Cruickshank, J. K., Vanhegan, R. I., Matthews, D. R., Cooper, G. J., Holman, R. R., and Turner, R. C. (1988) Islet amyloid, increased A-cells, reduced B-cells and exocrine fibrosis: Quantitative changes in the pancreas in type 2 diabetes, *Diabetes Res. 9*, 151−159.

8. Kloppel, G., Lohr, M., Habich, K., Oberholzer, M., and Heitz, P. U. (1985) Islet pathology and the pathogenesis of type 1 and type 2 diabetes mellitus revisited, *Surv. Synth. Pathol. Res. 4*, 110−125.
9. Stefan, Y., Orci, L., Malaisse-Lagae, F., Perrelet, A., Patel, Y., and Unger, R. H. (1982) Quantitation of endocrine cell content in the pancreas of nondiabetic and diabetic humans, *Diabetes 31*, 694−700.
10. Butler, A. E., Janson, J., Bonner-Weir, S., Ritzel, R., Rizza, R. A., and Butler, P. C. (2003) β-Cell deficit and increased β-cell apoptosis in humans with type 2 diabetes, *Diabetes 52*, 102−110.
11. Yoon, K. H., Ko, S. H., Cho, J. H., Lee, J. M., Ahn, Y. B., Song, K. H., Yoo, S. J., Kang, M. I., Cha, B. Y., Lee, K. W., Son, H. Y., Kang, S. K., Kim, H. S., Lee, I. K., and Bonner-Weir, S. (2003) Selective β-cell loss and α-cell expansion in patients with type 2 diabetes mellitus in Korea, *J. Clin. Endocrinol. Metab. 88*, 2300−2308.
12. Bernard, C., Berthault, M.-F., Saulnier, C., and Ktorza, A. (1999) Neogenesis vs. apoptosis as main components of pancreatic β-cell mass changes in glucose-infused normal and mildly diabetic adult rats, *FASEB J. 13*, 1195−1205.
13. Vinik, A., Rafaeloff, R., Pittenger, G., Rosenberg, L., and Duguid, W. (1997) Induction of pancreatic islet neogenesis, *Horm. Metab. Res. 29*, 278−293.
14. Butler, A. E., Janson, J., Soeller, W. C., and Butler, P. C. (2003) Increased β-cell apoptosis prevents adaptive increase in β-cell mass in mouse model of type 2 diabetes: Evidence for role of islet amyloid formation rather than direct action of am, *Diabetes 52*, 2304−2314.
15. Oyadomari, S., Koizumi, A., Takeda, K., Gotoh, T., Akira, S., Araki, E., and Mori, M. (2002) Targeted disruption of the CHOP gene delays endoplasmic reticulum stress-mediated diabetes, *J. Clin. Invest. 109*, 525−532.
16. Pick, A., Clark, J., Kubstrup, C., Levisetti, M., Pugh, W., Bonner-Weir, S., and Polonsky, K. S. (1998) Role of apoptosis in failure of β-cell mass compensation for insulin resistance and β-cell defects in the male Zucker diabetic fatty rat, *Diabetes 47*, 358−364.
17. Cerasi, E., Kaiser, N., and Leibowitz, G. (2000) Type 2 diabetes and β cell apoptosis, *Diabetes Metab. 26*, 13−16.
18. Chandra, J., Zhivotovsky, B., Zaitsev, S., Juntti-Berggren, L., Berggren, P., and Orrenius, S. (2001) Role of apoptosis in pancreatic β-cell death in diabetes, *Diabetes 50*, S44−S47.
19. Mandrup-Poulsen, T. (2001) β-Cell apoptosis: Stimuli and signaling, *Diabetes 50*, S58−S63.
20. Sesti, G. (2002) Apoptosis in the β cells: Cause or consequence of insulin secretion defect in diabetes? *Ann. Med. 34*, 444−450.
21. Oyadomari, S., Araki, E., and Mori, M. (2002) Endoplasmic reticulum stress-mediated apoptosis in pancreatic β-cells, *Apoptosis 7*, 335−345.
22. Diaz-Horta, O., Kamagate, A., Herchuelz, A., and Van Eylen, F. (2002) Na/Ca exchanger overexpression induces endoplasmic reticulum-related apoptosis and caspase-12 activation in insulin-releasing BRIN-BD11 cells, *Diabetes 51*, 1815−1824.
23. Mehmet, H. (2000) Caspases find a new place to hide, *Nature 403*, 29−30.
24. Bitko, V., and Barik, S. (2001) An endoplasmic reticulum-specific stress-activated caspase (caspase-12) is implicated in the apoptosis of A549 epithelial cells by respiratory syncytial virus, *J. Cell. Biochem. 80*, 441−454.
25. Nakagawa, T., Zhu, H., Morishima, N., Li, E., Xu, J., Yankner, B., and Yuan, J. (2000) Caspase-12 mediates endoplasmic-reticulum-specific apoptosis and cytotoxicity by amyloid-β, *Nature 403*, 98−103.
26. Rao, R. V., Castro-Obregon, S., Frankowski, H., Schuler, M., Stoka, V., del Rio, G., Bredesen, D. E., and Ellerby, H. M. (2002) Coupling endoplasmic reticulum stress to the cell death program. An Apaf-1-independent intrinsic pathway, *J. Biol. Chem. 277*, 21836−21842.
27. Aridor, M., and Balch, W. E. (1999) Integration of endoplasmic reticulum signaling in health and disease, *Nat. Med. 5*, 745−751.
28. Ron, D. (2002) Translational control in the endoplasmic reticulum stress response, *J. Clin. Invest. 110*, 1383−1388.
29. Harding, H. P., and Ron, D. (2002) Endoplasmic Reticulum Stress and the Development of Diabetes: A Review, *Diabetes 51*, S455−S461.
30. Cohen, G. M. (1997) Caspases: The executioners of apoptosis, *Biochem. J. 326*, 1−16.
31. Kaufman, R. J. (1999) Stress signaling from the lumen of the endoplasmic reticulum: Coordination of gene transcriptional and translational controls, *Genes Dev. 13*, 1211−1233.
32. Harding, H. P., Zeng, H., Zhang, Y., Jungries, R., Chung, P., Plesken, H., Sabatini, D. D., and Ron, D. (2001) Diabetes mellitus and exocrine pancreatic dysfunction in PERK$^{-/-}$ mice reveals a role for translational control in secretory cell survival, *Cell Press 7*, 1153−1163.
33. Delepine, M., Nicolino, M., Barrett, T., Golamaully, M., Lathrop, G. M., and Julier, C. (2000) EIF2AK3, encoding translation initiation factor 2-α kinase 3, is mutated in patients with Wolcott-Rallison syndrome, *Nat. Genet. 25*, 406.
34. Takeda, K., Inoue, H., Tanizawa, Y., Matsuzaki, Y., Oba, J., Watanabe, Y., Shinoda, K., and Oka, Y. (2001) WFS1 (Wolfram syndrome 1) gene product: Predominant subcellular localization to endoplasmic reticulum in cultured cells and neuronal expression in rat brain, *Hum. Mol. Genet. 10*, 477−484.
35. Araki, E., Oyadomari, S., and Mori, M. (2003) Impact of endoplasmic reticulum stress pathway on pancreatic β-cells and diabetes mellitus, *Exp. Biol. Med. 228*, 1213−1217.
36. Zinszner, H., Kuroda, M., Wang, X., Batchvarova, N., Lightfoot, R. T., Remotti, H., Stevens, J. L., and Ron, D. (1998) CHOP is implicated in programmed cell death in response to impaired function of the endoplasmic reticulum, *Genes Dev. 12*, 982−995.
37. Araki, E., Oyadomari, S., and Mori, M. (2003) Endoplasmic reticulum stress and diabetes mellitus, *Intern. Med. 42*, 7−14.
38. Thastrup, O., Dawson, A. P., Scharff, O., Foder, B., Cullen, P. J., Drobak, B. K., Bjerrum, P. J., Christensen, S. B., and Hanley, M. R. (1994) Thapsigargin, a novel molecular probe for studying intracellular calcium release and storage. 1989, *Agents Actions 43*, 187−193.
39. Zhou, Y.-P., Teng, D., Dralyuk, F., Ostrega, D., Roe, M. W., Philipson, L., and Polonsky, K. S. (1998) Apoptosis in insulin-secreting cells. Evidence for the role of intracellular Ca^{2+} stores and arachidonic acid metabolism, *J. Clin. Invest. 101*, 1623−1632.
40. Nowatzke, W., Ramanadham, S., Ma, Z., Hsu, F. F., Bohrer, A., and Turk, J. (1998) Mass spectrometric evidence that agents that cause loss of Ca^{2+} from intracellular compartments induce hydrolysis of arachidonic acid from pancreatic islet membrane phospholipids by a mechanism that does not require a rise in cytosolic Ca^{2+} concentration, *Endocrinology 139*, 4073−4085.
41. Gijon, M. A., and Leslie, C. C. (1997) Phospholipases A_2, *Semin. Cell Dev. Biol. 8*, 297−303.
42. Schaloske, R. H., and Dennis, E. A. (2007) The phospholipase A_2 superfamily and its group numbering system, *Biochim. Biophys. Acta* (in press).
43. Ma, Z., Ramanadham, S., Wohltmann, M., Bohrer, A., Hsu, F. F., and Turk, J. (2001) Studies of insulin secretory responses and of arachidonic acid incorporation into phospholipids of stably transfected insulinoma cells that overexpress group VIA phospholipase A_2 (iPLA$_2\beta$) indicate a signaling rather than a housekeeping role for iPLA$_2\beta$, *J. Biol. Chem. 276*, 13198−13208.
44. Mancuso, D. J., Jenkins, C. M., and Gross, R. W. (2000) The genomic organization, complete mRNA sequence, cloning, and expression of a novel human intracellular membrane-associated calcium-independent phospholipase A_2, *J. Biol. Chem. 275*, 9937−9945.
45. Tanaka, H., Takeya, R., and Sumimoto, H. (2000) A novel intracellular membrane-bound calcium-independent phospholipase A_2, *Biochem. Biophys. Res. Commun. 272*, 320−326.
46. Ma, Z., Ramanadham, S., Kempe, K., Chi, X. S., Ladenson, J., and Turk, J. (1997) Pancreatic islets express a Ca^{2+}-independent phospholipase A_2 enzyme that contains a repeated structural motif homologous to the integral membrane protein binding domain of ankyrin, *J. Biol. Chem. 272*, 11118−11127.
47. Balsinde, J., Bianco, I. D., Ackermann, E. J., Conde-Frieboes, K., and Dennis, E. A. (1995) Inhibition of calcium-independent phospholipase A_2 prevents arachidonic acid incorporation and phospholipid remodeling in P388D1 macrophages, *Proc. Natl. Acad. Sci. U.S.A. 92*, 8527−8531.
48. Boilard, E., and Surette, M. E. (2001) Anti-CD3 and concanavalin A-induced human t cell proliferation is associated with an increased rate of arachidonate-phospholipid remodeling. Lack of involvement of group IV and group VI phospholipase A_2 in remodeling and increased susceptibility of proliferating T cells to CoA-independent transacylase inhibitor-induced apoptosis, *J. Biol. Chem. 276*, 17568−17575.

49. Isenovic, E., and LaPointe, M. C. (2000) Role of Ca^{2+}-Independent Phospholipase A_2 in the Regulation of Inducible Nitric Oxide Synthase in Cardiac Myocytes, *Hypertension 35*, 249−254.
50. Maggi, L. B., Jr., Moran, J. M., Scarim, A. L., Ford, D. A., Yoon, J.-W., McHowat, J., Buller, R. M. L., and Corbett, J. A. (2002) Novel role for calcium-independent phospholipase A_2 in the macrophage antiviral response of inducible nitric-oxide synthase expression, *J. Biol. Chem. 277*, 38449−38455.
51. Tithof, P. K., Olivero, J., Ruehle, K., and Ganey, P. E. (2000) Activation of neutrophil calcium-dependent and -independent phospholipases A_2 by organochlorine compounds, *Toxicol. Sci. 53*, 40−47.
52. Williams, S. D., and Ford, D. A. (2001) Calcium-independent phospholipase A_2 mediates CREB phosphorylation and c-fos expression during ischemia, *Am. J. Physiol. 281*, H168−H176.
53. Moran, J. M., Buller, R. M. L., McHowat, J., Turk, J., Wohltmann, M., Gross, R. W., and Corbett, J. A. (2005) Genetic and pharmacologic evidence that calcium-independent phospholipase $A_2\beta$ regulates virus-induced inducible nitric-oxide synthase expression by macrophages, *J. Biol. Chem. 280*, 28162−28168.
54. Ramanadham, S., Hsu, F.-F., Bohrer, A., Ma, Z., and Turk, J. (1999) Studies of the role of group vi phospholipase A_2 in fatty acid incorporation, phospholipid remodeling, lysophosphatidylcholine generation, and secretagogue-induced arachidonic acid release in pancreatic islets and insulinoma cells, *J. Biol. Chem. 274*, 13915−13927.
55. Ramanadham, S., Song, H., Hsu, F. F., Zhang, S., Crankshaw, M., Grant, G. A., Newgard, C. B., Bao, S., Ma, Z., and Turk, J. (2003) Pancreatic islets and insulinoma cells express a novel isoform of group VIA phospholipase A_2 ($iPLA_2\beta$) that participates in glucose-stimulated insulin secretion and is not produced by alternate splicing of the $iPLA_2\beta$ transcript, *Biochemistry 42*, 13929−13940.
56. Atsumi, G.-i., Tajima, M., Hadano, A., Nakatani, Y., Murakami, M., and Kudo, I. (1998) Fas-induced arachidonic acid release is mediated by Ca^{2+}-independent phospholipase A_2 but not cytosolic phospholipase A_2, which undergoes proteolytic inactivation, *J. Biol. Chem. 273*, 13870−13877.
57. Atsumi, G.-i., Murakami, M., Kojima, K., Hadano, A., Tajima, M., and Kudo, I. (2000) Distinct roles of two intracellular phospholipase A_2s in fatty acid release in the cell death pathway. Proteolytic fragment of type IVA cytosolic phospholipase $A_2\alpha$ inhibits stimulus-induced arachidonate release, whereas that of type VI Ca^{2+}-independent phospholipase A_2 augments spontaneous fatty acid release, *J. Biol. Chem. 275*, 18248−18258.
58. Wilson, H. A., Allred, D. V., O'Neill, K., and Bell, J. D. (2000) Activities and interactions among phospholipases A_2 during thapsigargin-induced S49 cell death, *Apoptosis 5*, 389−396.
59. Shin, K. J., Chung, C., Hwang, Y. A., Kim, S. H., Han, M. S., Ryu, S. H., and Suh, P. (2002) Phospholipase A_2-mediated Ca^{2+} influx by 2,2′,4,6-tetrachlorobiphenyl in PC12 cells, *Toxicol. Appl. Pharmacol. 78*, 37−43.
60. Tithof, P. K., Elgayyar, M., Cho, Y., Guan, W. E. I., Fisher, A. B., and Peters-Golden, M. (2002) Polycyclic aromatic hydrocarbons present in cigarette smoke cause endothelial cell apoptosis by a phospholipase A_2-dependent mechanism, *FASEB J. 16*, 1463−1464.
61. Gross, R. W., Ramanadham, S., Kruszka, K. K., Han, X., and Turk, J. (1993) Rat and human pancreatic islet cells contain a calcium ion independent phospholipase A_2 activity selective for hydrolysis of arachidonate which is stimulated by adenosine triphosphate and is specifically localized to islet β-cells, *Biochemistry 32*, 327−336.
62. Ramanadham, S., Gross, R. W., Han, X., and Turk, J. (1993) Inhibition of arachidonate release by secretagogue-stimulated pancreatic islets suppresses both insulin secretion and the rise in β-cell cytosolic calcium ion concentration, *Biochemistry 32*, 337−346.
63. Ramanadham, S., Hsu, F. F., Zhang, S., Jin, C., Bohrer, A., Song, H., Bao, S., Ma, Z., and Turk, J. (2004) Apoptosis of insulin-secreting cells induced by endoplasmic reticulum stress is amplified by overexpression of group VIA calcium-independent phospholipase A_2 ($iPLA_2\beta$) and suppressed by inhibition of $iPLA_2\beta$, *Biochemistry 43*, 918−930.
64. Jayadev, S., Liu, B., Bielawska, A. E., Lee, J. Y., Nazaire, F., Pushkareva, M. Y., Obeid, L. M., and Hannun, Y. A. (1995) Role for ceramide in cell cycle arrest, *J. Biol. Chem. 270*, 2047−2052.
65. Obeid, L. M., and Hannun, Y. A. (1995) Ceramide: A stress signal and mediator of growth suppression and apoptosis, *J. Cell. Biochem. 58*, 191−198.
66. Venable, M. E., Lee, J. Y., Smyth, M. J., Bielawska, A., and Obeid, L. M. (1995) Role of ceramide in cellular senescence, *J. Biol. Chem. 270*, 30701−30708.
67. Coffin, J. M., and Hart, G. W. (1996) *Retrovirus*, Cold Spring Harbor Laboratory Press, Plainview, NY.
68. Ma, Z., Zhang, S., Turk, J., and Ramanadham, S. (2002) Stimulation of insulin secretion and associated nuclear accumulation of $iPLA_2\beta$ in INS-1 insulinoma cells, *Am. J. Physiol. 282*, E820−E833.
69. Dallner, G. (1974) Isolation of rough and smooth microsomes: General, *Methods Enzymol. 31* (Part A), 191−201.
70. Depierre, J. W., and Dallner, G. (1976) *Isolation, subfractionation, and characterization of the endoplasmic reticulum*, Vol. 3, John Wiley, New York.
71. Desagher, S., Osen-Sand, A., Nichols, A., Eskes, R., Montessuit, S., Lauper, S., Maundrell, K., Antonsson, B., and Martinou, J.-C. (1999) Bid-induced conformational change of Bax is responsible for mitochondrial cytochrome c release during apoptosis, *J. Cell Biol. 144*, 891−901.
72. Hsu, F. F., and Turk, J. (2002) Characterization of ceramides by low energy collisional-activated dissociation tandem mass spectrometry with negative-ion electrospray ionization, *J. Am. Soc. Mass Spectrom. 13*, 558−570.
73. Hsu, F. F., Turk, J., Stewart, M. E., and Downing, D. T. (2002) Structural studies on ceramides as lithiated adducts by low energy collisional-activated dissociation tandem mass spectrometry with electrospray ionization, *J. Am. Soc. Mass Spectrom. 13*, 680−695.
74. Hsu, F. F., and Turk, J. (2000) Structural determination of sphingomyelin by tandem mass spectrometry with electrospray ionization, *J. Am. Soc. Mass Spectrom. 11*, 437−449.
75. Bao, S., Miller, D. J., Ma, Z., Wohltmann, M., Eng, G., Ramanadham, S., Moley, K., and Turk, J. (2004) Male mice that do not express group via phospholipase A_2 produce spermatozoa with impaired motility and have greatly reduced fertility, *J. Biol. Chem. 279*, 38194−38200.
76. Nicholson, D. W., and Thornberry, N. A. (1997) Caspases: Killer proteases, *Trends Biochem. Sci. 22*, 299−306.
77. Oliver, F. J., de la Rubia, G., Rolli, V., Ruiz-Ruiz, M. C., de Murcia, G., and Murcia, J. M.-d. (1998) Importance of poly(ADP-ribose) polymerase and its cleavage in apoptosis. Lesson from an uncleavable mutant, *J. Biol. Chem. 273*, 33533−33539.
78. Marchesini, N., Luberto, C., and Hannun, Y. A. (2003) Biochemical properties of mammalian neutral sphingomyelinase2 and its role in sphingolipid metabolism, *J. Biol. Chem. 278*, 13775−13783.
79. Shimabukuro, M., Higa, M., Zhou, Y.-T., Wang, M.-Y., Newgard, C. B., and Unger, R. H. (1998) Lipoapoptosis in β-cells of obese prediabetic fa/fa rats. Role of serine palmitoyltransferase overexpression, *J. Biol. Chem. 273*, 32487−32490.
80. Fonseca, S. G., Fukuma, M., Lipson, K. L., Nguyen, L. X., Allen, J. R., Oka, Y., and Urano, F. (2005) WFS1 is a novel component of the unfolded protein response and maintains homeostasis of the endoplasmic reticulum in pancreatic β-cells, *J. Biol. Chem. 280*, 39609−39615.
81. Ueda, K., Kawano, J., Takeda, K., Yujiri, T., Tanabe, K., Anno, T., Akiyama, M., Nozaki, J., Yoshinaga, T., Koizumi, A., Shinoda, K., Oka, Y., and Tanizawa, Y. (2005) Endoplasmic reticulum stress induces WFS1 gene expression in pancreatic β-cells via transcriptional activation, *Eur. J. Endocrinol. 153*, 167−176.
82. Yamada, T., Ishihara, H., Tamura, A., Takahashi, R., Yamaguchi, S., Takei, D., Tokita, A., Satake, C., Tashiro, F., Katagiri, H., Aburatani, H., Miyazaki, J.-i., and Oka, Y. (2006) WFS1-deficiency increases endoplasmic reticulum stress, impairs cell cycle progression and triggers the apoptotic pathway specifically in pancreatic β-cells, *Hum. Mol. Genet. 15*, 1600−1609.
83. Socha, L., Silva, D., Lesage, S., Goodnow, C., and Petrovsky, N. (2003) The role of endoplasmic reticulum stress in nonimmune diabetes: NOD.k iHEL, a novel model of β-cell death, *Ann. N.Y. Acad. Sci. 1005*, 178−183.
84. Hannun, Y. A. (1994) The sphingomyelin cycle and the second messenger function of ceramide, *J. Biol. Chem. 269*, 3125−3128.
85. Franzen, R., Fabbro, D., Aschrafi, A., Pfeilschifter, J., and Huwiler, A. (2002) Nitric oxide induces degradation of the neutral ceramidase in rat renal mesangial cells and is counterregulated by protein kinase, *J. Biol. Chem. 277*, 46184−46190.

86. Kelpe, C. L., Moore, P. C., Parazzoli, S. D., Wicksteed, B., Rhodes, C. J., and Poitout, V. (2003) Palmitate inhibition of insulin gene expression is mediated at the transcriptional level via ceramide synthesis, *J. Biol. Chem. 278*, 30015−30021.
87. Lupi, R., Dotta, F., Marselli, L., Del, Guerra, S., Masini, M., Santangelo, C., Patane, G., Boggi, U., Piro, S., Anello, M., Bergamini, E., Mosca, F., Di Mario, U., Del Prato, S., and Marchetti, P. (2002) Prolonged exposure to free fatty acids has cytostatic and pro-apoptotic effects on human pancreatic islets: Evidence that β-cell death is caspase mediated, partially dependent on ceramide pathway, and Bcl-2 regulated, *Diabetes 51*, 1437−1442.
88. Becker, K. P., Kitatani, K., Idkowiak-Baldys, J., Bielawski, J., and Hannun, Y. A. (2005) Selective inhibition of juxtanuclear translocation of protein kinase c βII by a negative feedback mechanism involving ceramide formed from the salvage pathway, *J. Biol. Chem. 280*, 2606−2612.
89. Holz, G. G., Leech, C. A., Heller, R. S., Castonguay, M., and Habener, J. F. (1999) cAMP-dependent mobilization of intracellular Ca^{2+} stores by activation of ryanodine receptors in pancreatic β-cells. A Ca^{2+} signaling system stimulated by the insulinotropic hormone glucagon-like peptide-1-(7−37), *J. Biol. Chem. 274*, 14147−14156.
90. Schievella, A. R., Regier, M. K., Smith, W. L., and Lin, L.-L. (1995) Calcium-mediated translocation of cytosolic phospholipase A_2 to the nuclear envelope and endoplasmic reticulum, *J. Biol. Chem. 270*, 30749−30754.
91. Ramanadham, S., Bohrer, A., Gross, R. W., and Turk, J. (1993) Mass spectrometric characterization of arachidonate-containing plasmalogens in human pancreatic islets and in rat islet β-cells and subcellular membranes, *Biochemistry 32*, 13499−13509.
92. Johns, D. G., and Webb, R. C. (1998) TNF-α-induced endothelium-independent vasodilation: A role for phospholipase A_2-dependent ceramide signaling, *Am. J. Physiol. 275*, H1592−H1598.
93. Robinson, B. S., Hii, C. S., Poulos, A., and Ferrante, A. (1997) Activation of neutral sphingomyelinase in human neutrophils by polyunsaturated fatty acids, *Immunology 91*, 274−280.
94. Taketo, M. M., and Sonoshita, M. (2002) Phospolipase A_2 and apoptosis, *Biochim. Biophys. Acta 1585*, 72−76.
95. Zager, R. A., Conrad, D. S., and Burkhart, K. (1998) Ceramide accumulation during oxidant renal tubular injury: Mechanisms and potential consequences, *J. Am. Soc. Nephrol. 9*, 1670−1680.
96. Marchesini, N., and Hannun, Y. A. (2004) Acid and neutral sphingomyelinases: Roles and mechanisms of regulation, *Biochem. Cell Biol. 82*, 27−44.
97. Fensome, A. C., Josephs, M., Katan, M., and Rodrigues-Lima, F. (2002) Biochemical identification of a neutral sphingomyelinase 1 (NSM1)-like enzyme as the major NSM activity in the DT40 B-cell line: Absence of a role in the apoptotic response to endoplasmic reticulum stress, *Biochem. J. 365*, 69−77.
98. Tamiya-Koizumi, K., Umekawa, H., Yoshida, S., and Kojima, K. (1989) Existence of Mg^{2+}-dependent, neutral sphingomyelinase in nuclei of rat ascites hepatoma cells, *J. Biochem. 106*, 593−598.
99. Jurivich, D. A., Sistonen, L., Sarge, K. D., and Morimoto, R. I. (1994) Arachidonate is a potent modulator of human heat shock gene transcription, *Proc. Natl. Acad. Sci. U.S.A. 91*, 2280−2284.
100. Ramanadham, S., Wolf, M. J., Jett, P. A., Gross, R. W., and Turk, J. (1994) Characterization of an ATP-stimulatable Ca^{2+}-independent phospholipase A_2 from clonal insulin-secreting HIT cells and rat pancreatic islets: A possible molecular component of the β-cell fuel sensor, *Biochemistry 33*, 7442−7452.
101. Tepper, A. D., Ruurs, P., Wiedmer, T., Sims, P. J., Borst, J., and van Blitterswijk, W. J. (2000) Sphingomyelin hydrolysis to ceramide during the execution phase of apoptosis results from phospholipid scrambling and alters cell-surface morphology, *J. Cell Biol. 150*, 155−164.

BI700017Z